This is a preprint, the final version is subject to change, of the American Mineralogist (MSA)
Cite as Authors (Year) Title. American Mineralogist, in press.
DOI: https://doi.org/10.2138/am-2018-6515

Revision 1

Comparison of Rietveld-compatible structureless fitting analysis methods for accurate quantification of carbon dioxide fixation in ultramafic mine tailings

Connor C. Turvey[1]*, Jessica L. Hamilton[1,2a] and Siobhan A. Wilson[1,3a]

[1]School of Earth, Atmosphere & Environment, Monash University, Clayton, Melbourne, Victoria 3800, Australia

[2]School of Earth and Environmental Sciences, The University of Queensland, St Lucia, QLD 4072, Australia

[3]Department of Earth and Atmospheric Sciences, University of Alberta, Edmonton, Alberta, T6G 2E3, Canada

*Corresponding author, connor.turvey@monash.edu, +61 03 9905 4382

[a] Current Address

This is a preprint, the final version is subject to change, of the American Mineralogist (MSA)
Cite as Authors (Year) Title. American Mineralogist, in press.
DOI: https://doi.org/10.2138/am-2018-6515

Abstract

The carbonation of ultramafic rocks, including tailings from ultramafic-hosted ore deposits, can be used to remove CO_2 from the atmosphere and store it safely within minerals over geologic time scales. Quantitative X-ray diffraction (XRD) using the Rietveld method can be employed to estimate the amount of carbon sequestered by carbonate minerals that form as a result of weathering of ultramafic rocks. However, the presence of structurally disordered phases such as serpentine minerals, which are common in ultramafic ore bodies such as at the Woodsreef chrysotile mine (NSW, Australia), results in samples that cannot be analysed using typical Rietveld refinement strategies. Previous investigations of carbon sequestration at Woodsreef and other ultramafic mine sites typically used modified Rietveld refinement methods that apply structureless pattern fitting for disordered phases; however, no detailed comparison of the accuracy (or precision) of these methods for carbon accounting has yet been done, making it difficult to determine the most appropriate analysis method. Such an analysis would need to test whether some methods more accurately quantify the abundances of certain minerals, such as pyroaurite [$Mg_6Fe^{3+}_2(CO_3)(OH)_{16}\cdot 4H_2O$] and other hydrotalcite group minerals, which suffer from severe preferred orientation and may play an important role in carbon sequestration at some mines. Here, we assess and compare the accuracy, and to a lesser extent the precision, of three different non-traditional Rietveld refinement methods for carbon accounting: (1) the PONKCS method, (2) the combined use of a Pawley fit for serpentine minerals and an internal standard (Pawley/internal standard method) and (3) the combined use of PONKCS and Pawley/internal standard methods. We examine which of these approaches represents the most accurate way to quantify the abundances of serpentine, pyroaurite and other carbonate-bearing phases in a given sample. We demonstrate that by combining the PONKCS and Pawley/internal standard methods it is possible to quantify the abundances of disordered phases in a sample and to obtain an estimate of the amorphous content and any unaccounted

intensity in an XRD pattern. Eight artificial tailings samples with known mineralogical compositions were prepared to reflect the natural variation found within the tailings at the Woodsreef chrysotile mine. Rietveld refinement results for the three methods were compared with the known compositions of each sample to calculate absolute and relative error values and to evaluate the accuracy of the three methods, including whether they produce systematic under- or overestimates of mineral abundance. Estimated standard deviations were also calculated during refinements; these values, which are a measure of precision, were not strongly affected by the choice of refinement method. The abundance of serpentine minerals is, however, systematically overestimated when using the PONKCS and Pawley/internal standard methods, and the abundances of minor phases (< 10 wt%) are systematically underestimated using all three methods. Refined abundances for pyroaurite were found to be increasingly susceptible to error with increasing abundance, with an underestimation of 6.6 wt% absolute (60.6 % relative) for a sample containing 10.9 wt% pyroaurite. These significant errors are due to difficulties in mitigating preferred orientation of hydrotalcite minerals during sample preparation as well as modelling its effects on XRD patterns. The abundances of hydromagnesite [$Mg_5(CO_3)_4(OH)_2 \cdot 4H_2O$], another important host for atmospheric CO_2 during weathering of ultramafic rocks, was consistently underestimated by all three methods, with the highest underestimation being 3.7 wt% absolute (or 25 % relative) for a sample containing 15 wt% hydromagnesite. Overall, the Pawley/internal standard method produced more accurate results than the PONKCS method, with an average bias per refinement of 6.7 wt%, compared with 10.3 wt% using PONKCS and 12.9 wt% for the combined PONKCS-Pawley/internal standard method. Furthermore, the values for refined abundance of hydromagnesite obtained from refinements using the Pawley/internal standard method were significantly more accurate than those for refinements done with the PONKCS method, with relative errors typically less than 25 % for hydromagnesite abundances between 5 and 15 wt%. The simpler and faster

sample preparation makes the PONKCS method well-suited for rapid carbon accounting, for instance in the field using a portable XRD; however, the superior accuracy gained when using an internal standard make the Pawley/internal standard method the preferable means of undertaking a detailed laboratory-based study. As all three methods displayed an underestimation of carbonate phases, applying these methods to natural samples will likely produce an underestimate of hydromagnesite and hydrotalcite group mineral abundances. As such, crystallographic accounting strategies that use modified Rietveld refinement methods produce a conservative estimate of the carbon sequestered in minerals.

Keywords: carbon accounting, X-ray diffraction, Rietveld analysis, PONKCS method, Pawley/internal standard method, serpentine, amorphous material, pyroaurite, hydromagnesite

Introduction

The release of anthropogenic CO_2 and other greenhouse gases into the atmosphere is causing potentially irreparable damage to the Earth's climate, with global temperature rises of between 1.5 and 2°C predicted before the end of the 21st century (Houghton et al., 2001; IPCC, 2005; IPCC, 2013; IPCC, 2014; Millar et al., 2017). This has led to the development of multiple strategies to combat the adverse impacts of anthropogenic climate change upon the planet, including the reduction of both deforestation and our reliance on fossil fuels, adoption of market controls on greenhouse gas emissions, increased use of renewable energy, and the use of carbon sequestration technologies (Cleugh et al., 2011; IPCC, 2013; IPCC, 2014; Pacala and Socolow, 2004). Carbon mineralisation is a carbon sequestration strategy that traps CO_2 within the crystal structures of minerals (Lackner, 2003; Lackner et al., 1995; Seifritz, 1990). Carbon mineralisation has been proposed for capturing carbon from waste streams of power plants as well as capturing it directly from the atmosphere through passive or accelerated carbonation of mine tailings and alkaline wastes (as reviewed by Bobicki et al, 2012; Chang et al., 2011;

Cleugh et al., 2011; Lackner, 2002; Leung et al., 2014; Oelkers., 2008; Power et al., 2013a; Power et al., 2013b). It has been predicted that over a timescale of 10^6 years, carbonate minerals will likely be the primary as sink for all anthropogenic CO_2 (Kump et al., 2000); however, carbon mineralisation reactions need to be accelerated to curb net greenhouse gas emissions on a socially relevant timescale.

Ultramafic rocks, and mine tailings in particular, are of great interest for use in enhanced passive carbonation (i.e., carbonation of rocks by reaction with atmospheric CO_2 at an enhanced rate) because they provide an ideal feedstock for the formation of carbonate minerals. Mg- and Ca-rich silicate and hydroxide minerals weather quickly when exposed to meteoric precipitation and atmospheric CO_2, releasing Mg^{2+} and Ca^{2+} into solution, where they react with aqueous carbonate anions to form hydrated carbonate minerals (Berner, 1990; Lackner, 2002; Oelkers et al., 2008; Power et al., 2013a). Furthermore, the mineral processing that tailings have undergone reduces grain size thereby increasing surface area and reactivity, ensuring that mineral dissolution and carbonation reactions occur over rapid time scales (Wilson et al., 2009a; Wilson et al., 2014). Previous research in this field has investigated the passive carbonation reactions that are occurring within the tailings material of several ultramafic mines in Australia, Canada and Norway (e.g., Assima et al., 2012; Bea et al., 2012; Beinlich and Austrheim, 2012; Hamilton et al., 2018; Hamilton et al., 2016; Hitch et al., 2010; Lechat et al., 2016; McCutcheon et al., 2015; McCutcheon et al., 2017; McCutcheon et al., 2016; Oskierski et al., 2013; Pronost et al., 2012; Pronost et al., 2011; Turvey et al., 2017; Wilson et al., 2009a; Wilson et al., 2014; Wilson et al., 2006; Wilson et al., 2009b). Laboratory and field trials are underway using abiotic and biological means of enhancing these reaction rates to maximize carbon sequestration in mine wastes (e.g., Assima et al., 2013a; Assima et al., 2014a; Assima et al., 2014b; Assima et al., 2012; Beaudoin et al., 2017; Harrison et al., 2015; Harrison et al., 2013; McCutcheon et al., 2017; McCutcheon et al., 2016).

This is a preprint, the final version is subject to change, of the American Mineralogist (MSA)
Cite as Authors (Year) Title. American Mineralogist, in press.
DOI: https://doi.org/10.2138/am-2018-6515

Quantifying the amount of atmospheric CO_2 that has been trapped within tailings storage facilities is an important first step in understanding their carbon sequestration potential and how much atmospheric CO_2 has already been sequestered (Wilson et al., 2009a; Wilson et al., 2014; Wilson et al., 2006). There are multiple methods for quantifying carbon fixation in minerals, which work best when used in combination. Typical bulk geochemical analyses can be used to quantify the amount of carbon stored within minerals in tailings but they cannot be used to differentiate between different carbonate-bearing phases, nor can they be used to distinguish between bedrock carbonate minerals and secondary carbonate minerals that have formed via passive capture of CO_2 from air. Stable and radiogenic isotopic fingerprinting can be used to trace the source of carbon in minerals but cannot be used to give a quantitative assessment of the amount CO_2 stored within a sample of tailings (Oskierski et al., 2013; Wilson et al., 2009a; Wilson et al., 2014). Textural observations, using microscopy, and isotopic analyses can be used in combination to determine the origin of each carbon-bearing mineral species, either as gangue minerals inherited from the ore or as an alteration phase derived from an atmospheric source of carbon (Oskierski et al., 2013; Wilson et al., 2009a; Wilson et al., 2014). Quantitative XRD can be used to provide an estimate of the weight-percent contribution of each gangue and secondary carbonate mineral in a sample of tailings, which can then be used in combination with textural and isotopic data to estimate the amount of atmospheric CO_2 sequestered in the tailings from stoichiometry (Wilson et al., 2006; Wilson et al., 2009a).

Performing quantitative XRD upon samples of ultramafic tailings is often challenging owing to the presence of serpentine minerals, other disordered minerals such as smectites, and amorphous phases (e.g., Mervine et al., in review; Turvey et al., 2017). Like many clay minerals, the serpentine polymorphs chrysotile, antigorite and lizardite, are affected by turbostratic stacking disorder and thus do not have well-defined crystal structures (Wicks and Whittaker, 1975). Amorphous silica and/or amorphous hydrated carbonate phases are also

products of carbon mineralisation reactions that have been identified in previous studies of passive and enhanced tailings carbonation both in the laboratory (Harrison et al., 2015) and in the field at Woodsreef (McCutcheon et al., 2017; Oskierski et al., 2013). Owing to the mineralogical complexity of ultramafic rocks, traditional Rietveld refinements using powder XRD data cannot be used for quantitative phase analysis. The original Rietveld method typically requires that all phases in a mixture have well-defined and well-ordered crystal structures (Bish and Howard, 1988; Hill and Howard, 1987; Rietveld, 1969). This has been overcome in previous studies by using alternative quantitative XRD methods or by using modified Rietveld refinement methods. Wilson et al. (2009b) and Oskierski et al. (2013) used the internal standard method of Alexander and Klug (1948) and the reference intensity ratio method (Chung, 1974) to quantify individual carbon-bearing alteration minerals in serpentinite mine tailings. Although the internal standard method and reference intensity ratio method can yield more accurate quantitative estimates of low-abundance carbonate minerals (Wilson et al., 2009b), these methods are laborious to calibrate; Rietveld refinement offers the advantage of simultaneous, complete quantification of all detectable phases in sample. Previous studies such Turvey et al. (2017) and Wilson et al. (2006) have instead used modified Rietveld methods, aiming to keep the advantages of the Rietveld method while introducing structureless pattern fitting to quantify disordered phases. Turvey et al. (2017) used the Partial Or No Known Crystal Structure (PONKCS; Scarlett & Madsen, 2006) method to model the peak profiles of serpentine minerals, whereas Wilson et al. (2006) applied structureless pattern fitting with the Pawley method (Pawley, 1981) and an internal standard so that serpentine minerals could be modelled and quantified as ‘amorphous phases’. These methods have begun to see adoption by the minerals industry for carbon accounting (e.g., Mervine et al., in review), but there has not previously been a direct comparison of the PONKCS and Pawley/internal standard methods and the accuracy and precision of the results that they produce. These methods also have the

potential to be applied simultaneously to quantify multiple disordered phases and amorphous phases separately (the latter without the need to create a PONKCS model) or as an estimate of the misfit between an XRD pattern and Rietveld refinement model for a sample.

The purpose of this study is four-fold. The primary objective of this work is to optimize a reproducible refinement strategy using artificial samples of serpentinite tailings that span a range of mineralogical compositions, so that this method can be applied with a high degree of accuracy to natural samples of similar composition. The second objective is to provide a direct comparison between two quantitative XRD methods, the PONKCS method (Scarlett and Madsen, 2006) and the Pawley/internal standard method (Wilson et al., 2006), when working with serpentinite tailings. This is achieved by analysis of eight artificial serpentinite tailings samples with known mineralogical compositions. The accuracy of the two methods can be assessed by comparing the known and refined values for mineral abundances. Thirdly, this study aims to assess whether the two methods can be successfully applied together to simultaneously quantify (1) multiple poorly ordered phases using PONKCS models and (2) the presence of any amorphous content or misfits caused by unaccounted for intensity in the patterns using an internal standard. Here, rather than add a known amount of an amorphous material to our samples, we use this method as a measure of misfit between our models and observed results. The fourth objective is to assess the accuracy of the PONKCS method, the Pawley/internal standard method and the combined use of these methods for quantifying the abundance of pyroaurite [$Mg_6Fe^{3+}_2(CO_3)(OH)_{16}\cdot 4H_2O$], the most common hydrotalcite supergroup mineral in serpentinite-hosted ore deposits and tailings storage facilities. Pyroaurite makes up a significant portion of the tailings material at Woodsreef, and it is likely to be trapping atmospheric CO_2 (Oskierski et al., 2013), thus accurately quantifying the abundance of pyroaurite is essential for successful carbon accounting at this site and at many other mines.

This is a preprint, the final version is subject to change, of the American Mineralogist (MSA)
Cite as Authors (Year) Title. American Mineralogist, in press.
DOI: https://doi.org/10.2138/am-2018-6515

Experimental Methods

Synthetic tailings samples

Eight synthetic tailings samples of known compositions were prepared to evaluate the accuracy of the three Rietveld refinement methods and to allow for the optimization of the refinement methods. The synthetic tailings were prepared to mimic the mineralogical variation found throughout the tailings storage facility of the Woodsreef chrysotile mine, a derelict mine in New South Wales, Australia, that is the subject of ongoing research for its carbonation potential. The tailings at the Woodsreef chrysotile mine have been undergoing passive carbon mineralisation by reaction with atmospheric CO_2 since mine closure in 1983 (Oskierski et al., 2013). The Woodsreef mine was Australia's largest tonnage chrysotile mine, producing 500,000 t of long-fibre chrysotile as well as 24 Mt of tailings and 75 Mt of waste rock during operation (Laughton and Green, 2002; Merril et al., 1980). Previous studies at Woodsreef have shown that multiple carbonate minerals are present in the tailings, including secondary pyroaurite and hydromagnesite [$Mg_5(CO_3)_4(OH)_2{\cdot}4H_2O$] as well as trace amounts of gangue calcite, magnesite and dolomite, and that the tailings mineralogy is dominated by the serpentine polymorphs, lizardite and chrysotile (McCutcheon et al., 2016; Oskierski et al., 2013; Turvey et al., 2017). The compositions of the artificial tailings samples were chosen to cover the full range of mineral abundances reported in the tailings at Woodsreef by Oskierski et al. (2013) and Turvey et al. (2017). These previous studies found that hydromagnesite was present at abundances <15 wt% and that the abundance of pyroaurite varied from 1 to 11 wt%. Known amounts of pure mineral specimens were weighed and mixed to produce the eight samples of synthetic tailings. See Table 1 for the compositions of the synthetic tailings samples. Samples Artrock1−4 were originally prepared for a previous study, Turvey et al. (2017), which investigated the potential use of portable XRD instruments and the PONKCS method for rapid,

field-based carbon accounting. No results are replicated between this study and Turvey et al. (2017) as different Rietveld refinement strategies were used here.

Insert Table 1 hereabouts.

Several specimens of serpentine were used as components within the synthetic tailings samples, Artrock1−8. The purity of the serpentine specimens was confirmed using X-ray powder diffraction and Raman spectroscopy. The dominant polymorph of serpentine within each sample was determined using XRD patterns and Raman spectra following the recommendations of Wicks (2000) and Rinaudo et al. (2003). The serpentine specimen used to make samples Artrock1−4 is a picrolite (chrysotile) taken from the Clinton Creek mine, Yukon, Canada (previously characterized by Wilson et al. 2006). The serpentine component of Artrocks5−8 consisted of lizardite [previously described by Wilson et al. (2009b)], sourced from the mineral collection of The University of British Columbia (original locality unknown). The hydromagnesite standard was taken from a carbonate playa near Atlin, British Columbia, Canada (07AT7-3; Power et al. 2014). The pyroaurite standard was produced by placing a natural sample of pulverized iowaite [$Mg_6Fe^{3+}_2Cl_2(OH)_{16}\cdot 4H_2O$] from the Mount Keith nickel mine, Western Australia in excess deionized water which was vigorously stirred for 48 hours. This method converts iowaite to pyroaurite through an anion exchange reaction using dissolved atmospheric CO_2 [adapted from the work of Bish (1980) and Miyata (1983)]. Following the exchange reaction Rietveld refinement indicated that the powder contained pyroaurite-3*R* (92.4 wt%), and minor amounts of brucite (2.2 wt%) and residual iowaite (5.4 wt%, also a 3*R* polytype). The magnetite standard sourced from the mineral collection at Monash University was found to be 94.4% pure by Rietveld refinement, with minor hematite (5.6 wt%) contamination.

All artificial tailings samples were milled for seven minutes under anhydrous ethanol using a McCrone micronizing mill to reduce the mean particle size and to ensure homogenization of the samples. Samples were dried at room temperature and disaggregated with an agate mortar and pestle prior to XRD analysis. A subsample of each micronized synthetic tailings sample was spiked using 10 wt% of an in-house fluorite standard for refinements using the Pawley/internal standard method and combined use of the PONKCS and Pawley/internal standard methods. The fluorite standard was determined to be 98.8 ± 3.3% crystalline by refinement of a 50:50 mixture by weight of the fluorite and NIST 676a α-Al_2O_3. Fluorite was used as an internal standard instead of corundum in order to minimise peak overlap between the internal standard and the sample. The 0 -1 4 corundum peak at 35.1° 2θ and, to a lesser extent, the 0 1 2 (25.5° 2θ) and -1 -1 0 (37.8° 2θ) peaks of corundum overlap with major peaks of serpentine minerals and magnetite. The diagnostic 1 1 1 and 2 0 2 fluorite peaks (at 28.3° 2θ and 47.0° 2θ, respectively) do not overlap with any peaks belonging to phases that are typically found in serpentinite mine tailings (the composition of which was used as the basis for the synthetic tailings samples).

Instrument details

XRD patterns of the synthetic tailings were collected using a Bruker D8 Advance X-ray diffractometer in the Monash X-ray Platform. Patterns were collected using a Cu X-ray tube operating at 40 kV and 40 mA, and a LynxEye 1D position sensitive detector operating over a 2θ range of 3−80° with a step size 0.02° and a dwell time of 1s/step. Samples were loaded into back loading cavity mounts against a frosted glass slide or 400 grit sandpaper to reduce preferred orientation of crystallites. Qualitative identification of minerals in the XRD patterns was performed using DIFFRAC.EVA V.2 (Bruker AXS) with reference to standard patterns from the ICDD PDF-2 database and Crystallography Open Database.

The contribution of instrumental peak broadening to XRD patterns collected from experimental samples was modelled using an instrument profile refined from a pattern of NIST SRM 660b LaB_6. Refinement of the LaB_6 pattern was done using the fundamental parameters approach (Cheary and Coehlo, 1992), which takes machine geometry into account, permitting an estimate of crystallite size and strain for specific minerals from refinements using XRD patterns collected from experimental samples.

Rietveld refinement strategy

Quantitative phase analysis was performed on the artificial tailings samples using the Rietveld method (Bish and Howard, 1988; Hill and Howard, 1987; Rietveld, 1969). Three modified approaches to the Rietveld method were employed: the PONKCS method (Scarlett and Madsen, 2006), the Pawley/internal standard method (Wilson et al., 2006) and a combined PONKCS Pawley/internal standard method. Rietveld refinements typically require that all phases in a mixture be well-ordered and have well-known crystal structures, as the mass and volume of the unit cell are used to derive a calibration factor that is used to quantify each phase (Bish and Howard, 1988). This makes quantifying mineral abundances in serpentinite tailings, such as those found at Woodsreef, and in the synthetic tailings, difficult because they are typically dominated by the presence of the serpentine polymorphs chrysotile and lizardite. Serpentine minerals, like many clay minerals, are affected by turbostratic stacking disorder, which leads to anisotropic peak broadening in XRD patterns and peaks that cannot be accurately modelled using traditional Rietveld refinements. These problems have previously been overcome by spiking the sample with an internal standard (Wilson et al., 2014; Wilson et al., 2006; Wilson et al., 2009b) and then using the Pawley method for structureless pattern fitting (Pawley, 1981), or by using the PONKCS method of Scarlett and Madsen (2006) as implemented for carbon accounting by Turvey et al. (2017).

Quantitative phase analysis via Rietveld refinement was performed using the XRD patterns of the synthetic tailings with DIFFRAC.TOPAS v.5 (Bruker AXS), using the fundamental parameters approach (Cheary and Coelho, 1992). Background was modelled using fourth-order Chebychev polynomials with an additional $1/x$ function. A default Brindley radius of 0.00025 mm and a packing density of 0.4 were used to correct for microabsorption contrast amongst all phases (Brindley, 1945). The sources of crystal structure information for all phases are shown in Table 2. The chrysotile and lizardite structures listed in Table 2 were then heavily modified, as described below, for implementation of the three refinement methods to allow for quantification of the serpentine minerals within the artificial tailings samples.

Insert Table 2 hereabouts

PONKCS method. The PONKCS method can be used to quantify the abundances of multiple disordered phases, such as serpentine minerals, without the addition of an internal standard into every sample. It is an external standard method in which one or more poorly crystalline phases are modelled using structureless profile fitting. The Rietveld refinement parameters Z, M and V are calibrated against those of an ordered, well-characterized phase, where Z=the number of formula units in the unit cell, M=the molecular mass of the formula unit and V=the unit cell volume (Scarlett and Madsen, 2006).

Two mixtures were made to create the PONKCS models for the two serpentine standards: a 50:50 wt% mix of NIST 676a α-Al_2O_3 corundum and chrysotile (from Clinton Creek, Yukon, Canada) and a 50:50 mix of NIST 676a α-Al_2O_3 and lizardite (sourced from The University of British Columbia). The space groups and unit cell parameters for lizardite and chrysotile were taken from Mellini and Viti (1994) and Falini et al. (2004), respectively. Calibrated mass (M) values for the unit cell of each disordered serpentine phase were obtained by Rietveld refinement for the two mixtures in DIFFRAC.TOPAS v.3 (Bruker AXS) using the Pawley

method for structureless pattern fitting (Pawley, 1981). Anisotropic peak shape exhibited by the serpentine minerals was modelled using the spherical harmonics approach of Stephens (1999). These refinements were used to generate Z and V values for the serpentine minerals, using Equation 1 below, where Z=the number of formula units in the unit cell, M=the molecular mass of the formula unit, V=the unit cell volume, S=the Rietveld scale factor and W=the weight fraction of the standard s and amorphous phase α. Combined with the Pawley method for structureless pattern fitting this created two PONKCS models that can be used in a similar manner to crystal structures when performing Rietveld refinements.

$$(ZV)_\alpha = \frac{W_\alpha}{W_s} \cdot \frac{S_s}{S_\alpha} \cdot \frac{(ZMV)_s}{M_\alpha} \quad (1)$$

Refinements were completed in a single step when using the PONKCS method for quantifying phases in serpentine-rich samples. Although PONKCS models were used for both lizardite and chrysotile, the refined abundances of these two phases was always summed to give a total abundance for serpentine minerals in line with the procedure that was employed in Turvey et al. (2017). Refinements were attempted using lizardite and chrysotile models individually but they were ultimately not used as they produced a worse fit (see below). The scale factors and unit cell parameters were allowed to refine for all phases. The Lorentzian crystallite size and strain values for pyroaurite, magnetite and hydromagnesite were allowed to refine from starting values of 1000 nm and 0.1, respectively. Crystallite size and strain were not refined for brucite as this phase was present at very low abundance and refining these values tended to lead to unrealistic peak broadening and unrealistically high refined abundances. A March-Dollase preferred orientation correction was used for the 0 0 3 peak of pyroaurite, 0 0 1 peak of brucite and 1 0 0 peak of hydromagnesite (using soft constraints to refine between values of 0.6 and 1). Asymmetrical peak shapes for the hydromagnesite were accounted for using a Thompson-Cox-Hasting pseudo-Voigt profile.

Pawley/internal standard method. Measuring the amorphous content of a sample by adding an internal standard and then performing Rietveld refinements was first proposed by (Bish and Howard, 1988). Gualtieri (2000) used the method to quantify the (amorphous) glass content of pyroclastic flows and Wilson et al. (2006) adapted the method to include structureless pattern fitting to treat disordered phases as though they were 'amorphous' for quantification of serpentine minerals. We used a 10 wt% spike of a well-ordered standard (an in-house fluorite standard) to quantify the amount of the disordered phases(s) in our samples. The amount of 'amorphous' material, X_a, can be calculated directly from the refined and known weights of the internal standard:

$$X_a = \left(\frac{100}{90}\right)\left[1 - \left(\frac{X_s}{X_{s,c}}\right)\right] \qquad (2)$$

where X_s is the measured weight of the internal standard and $X_{s,c}$ is the refined weight of the internal standard (Gualtieri, 2000). The Pawley method (Pawley, 1981) was used to extract peak intensities independently of the scattering structure model from powder diffraction patterns of pure chrysotile and lizardite samples. The extracted intensities with appropriate space groups and unit cell dimensions of chrysotile and lizardite were used to fit the serpentine component in the patterns for the artificial tailings samples as a peaks phase as used in Wilson et al. (2006).

A similar refinement strategy was used for the Pawley/internal standard method as for the PONKCS method. A chrysotile peaks phase was used to fit the peaks of all serpentine minerals present in all of the samples (see below). Refinements were attempted using both lizardite and chrysotile peaks phases but these results were ultimately not used as they produced a worse fit. Serpentine mineral abundance was calculated using Eq.2 based on the addition of 10 wt% fluorite. Scale factors and unit-cell parameters were refined for all phases in the sample. The Lorentzian crystallite size and strain values for pyroaurite, brucite, magnetite and

hydromagnesite were allowed to refine from starting values of 1000 nm and 0.1 respectively (refining to values of between 60 and 10000 nm, and 0.001−0.2 respectively). The Lorentzian crystallite size and strain values for the fluorite spike were held constant at 1000 nm and 0.1. A March-Dollase preferred orientation correction was used for the 0 0 3 peak of pyroaurite, 0 0 1 peak of brucite and 1 0 0 peak of hydromagnesite (refining between values of 0.6 and 1). Asymmetrical peak shapes for hydromagnesite were accounted for using a Thompson-Cox-Hasting pseudo-Voigt profile.

PONKCS Pawley/internal standard method. We used the PONKCS method to quantify the abundances of serpentine minerals while also including a 10 wt% fluorite internal standard to measure the abundance of any amorphous material in the synthetic tailings samples and estimate the misfit between unaccounted for intensity and the refinement. The Pawley/internal standard method can be used to quantify the abundances of any number of disordered or amorphous phases or can be used to give an estimate for unaccounted for intensity in the pattern; however, all these abundances are amalgamated and reported together only as 'amorphous content', it cannot be used to separate the individual abundances of multiple amorphous phases, and it cannot provide a separate estimate of how much material is unaccounted for in the model (Wilson et al., 2006). Low-abundance amorphous phases that do not produce Bragg peaks can be quantified using an internal standard without applying a peak fitting procedure (Bish and Howard, 1988; Gualtieri, 2000). The PONKCS method allows for individual disordered phases to be quantified in a sample but requires that a high-purity sample of the material exists that can be used to produce a suitable peaks phase and calibrated values of Z, M, and V (Scarlett and Madsen, 2006). Combining the method of Bish and Howard (1988) and Gualtieri (2000) with that of Scarlett and Madsen (2006) has the potential to overcome some of the shortcomings associated with each method and could be used to estimate how much crystalline and amorphous material remains unaccounted for in a refinement. It could also potentially be used

to quantify multiple separate disordered phases in cases where it is difficult to produce a PONKCS model for all such phases.

XRD patterns were collected from subsamples of the synthetic tailings that contained 10 wt% fluorite. No amorphous material was added to these samples. Instead, the estimate provided for 'amorphous' content using Eq.2 was used to test whether this method can be (1) used to accurately determine whether a sample contains no or a low amount of amorphous material and (2) used as a measure of goodness of fit in refinements employing PONKCS models. Rietveld refinements were performed in Topas.V5 using the structures outlined in Table 2, including chrysotile and lizardite structures that were used to produce structureless PONKCS models (see above). The fluorite internal standard was modelled using the same method as in the Pawley/internal standard method (see above), with the refined abundance of the internal standard was normalized to 10 wt%. Most of the phases in the artificial tailings (pyroaurite, magnetite, fluorite, brucite and hydromagnesite) were modelled using a standard Rietveld approach that relies upon structural information, whereas the peaks of the serpentine minerals (chrysotile and lizardite) were fitted using PONKCS models, and the abundance of 'amorphous' material was estimated using Eq.2.

PONKCS models were used for lizardite and chrysotile and the refined abundances for these two phases were summed to give a serpentine abundance (see section below). The crystallite size and strain values for the fluorite spike were kept constant at 1000 nm and 0.1 (as with the Pawley/internal standard method above) and a split-Pearson VII function was used to model the peak shape because it gave an improved fit compared with the fundamental parameters approach. All other refinement parameters were the same as those used in the PONKCS and Pawley/internal standard methods as outlined above, including refining scale factors and unit cell parameters, and Lorentzian size and strain for most phases; the use of a Thompson-Cox-Hastings pseudo-Voigt profile for modelling asymmetrical peak shape in hydromagnesite; and

the use of a March-Dollase preferred orientation correction for pyroaurite, brucite and hydromagnesite.

Serpentine Structures

Multiple refinement approaches were tested with all three methodologies to quantify the abundances of serpentine minerals within the artificial tailings. Refinements were done using structureless fitting models for (1) chrysotile, (2) lizardite and (3) both chrysotile and lizardite, with the individual abundances summed to model the overall serpentine abundance in the latter case, in order to determine whether the use of one or more of these models improved the accuracy of estimates for serpentine abundance. Ultimately, it was found that using both chrysotile and lizardite models produced more accurate estimates of mineral abundance and better fits when applying the PONKCS method (and combined PONKCS Pawley/internal standard method), even in cases where only one of these minerals was present in a sample. Using only the structureless model for chrysotile with the Pawley/internal standard method gave more accurate mineral abundance results than the combined use of both structureless models, including for Artrocks 5−8, which contained only lizardite. This indifference to the serpentine model that is used most likely occurs because the structureless pattern fitting procedure used here, which employs a spherical harmonics model for anisotropic peak shape (Stephens, 1999), is intended to be able to fit almost any peak shape. Lizardite and chrysotile (but not the third polymorph, antigorite) produce XRD patterns that are very similar with almost complete overlap of all major reflections (Wicks, 2000). This means that either the structureless model for lizardite or chrysotile can be used to fit the patterns produced by each of these serpentine polymorphs.

Preferred Orientation

In addition to the serpentine minerals, the abundances of several other minerals found in ultramafic rocks are also challenging to quantify accurately because these minerals suffer from severe preferred orientation. These phases include pyroaurite, iowaite and brucite. Preferred orientation occurs where platy or fibrous minerals preferentially align along certain crystallographic directions. This can lead to a drastic increase in the intensity of some reflections for a given zone or zones, with similar decreases in other reflections, which can result in over- or under-reporting of mineral abundances when using Rietveld refinement. Various preferred orientation corrections have been developed to account for this phenomenon including the March-Dollase correction (Dollase, 1986; Leventouri, 1997; March, 1932) and a spherical harmonics correction (Von Dreele, 1997). Back- or side-mounting techniques can also be employed during sample preparation to reduce the effects of preferred orientation. In this case, we re-collected patterns for the artificial tailings samples that exhibited the most severe preferred orientation by back-loading them against 400 grit sand paper rather than back-loading against frosted glass (which was used for samples that displayed a lesser degree of preferred orientation). This was deemed necessary even though it can introduce more complications in the form of surface roughness which can affect microabsorption.

For the purposes of this study, both the March-Dollase correction and a spherical harmonics correction were tested as methods to overcome the issues associated with quantifying the abundance of minerals that exhibited preferred orientation. Refinements using a spherical harmonics correction for preferred orientation tended to produce physically impossible results such as negative intensities, an undesirable occurrence that has been previously documented (Whitfield, 2008), as such the spherical harmonics correction for preferred orientation was ultimately discarded in favour of using the March-Dollase correction. Applying the March-Dollase correction on the 0 0 3*l* peaks for pyroaurite and iowaite (where present at trace

abundance), the 0 0 *l* peaks for brucite and the *h* 0 0 peaks for hydromagnesite, gave the best results. The degree of preferred orientation exhibited by the 0 0 3 pyroaurite peak and its higher orders reflections was most pronounced in the artificial samples with the highest weighed abundances for pyroaurite (e.g., 10.9 wt% pyroaurite in Artrock8). In these cases, the March-Dollase preferred orientation correction could be used to fit the peak intensities but the degree of correction necessary to achieve a very good fit to the 0 0 3 peak resulted in drastic underreporting of the pyroaurite abundance: in one case by up to 8.5 wt% (78.0 % relative error, as seen in Figure 1). Placing limits on the minimum and maximum values for the March-Dollase correction yielded more accurate refined abundances of pyroaurite but it led to a worse fit between the model and the observed intensities of the pyroaurite peaks, and a worse fit to the XRD pattern overall. Several variations were tested both for the PONKCS method and the Pawley/internal standard method, including using the March-Dollase correction with different lower limits used (e.g., a maximum value of 1 with a minimum of 0.6; a maximum value of 1 with a minimum value of 0.75). Figures 1 and 2 compare the resulting R_{wp} and refined pyroaurite abundances obtained using both methods and the different lower bounds for the March-Dollase correction. The refined value for the March-Dollase correction used on the 0 0 3l reflections of pyroaurite consistently reached the minimum value of 0.6 whenever minimum limits were set. When minimum values were not set, the refined values reached lower limits of 0.53 (when using the Pawley/internal standard method) and 0.47 (when using the PONKCS method). Ultimately, a minimum value of 0.6 provided a suitable compromise between (1) a good fit between the model and data and (2) the accuracy of the reported abundances for hydrotalcite minerals.

The McCrone micronizing mill that we used had been kept in good repair (with the rubber "mounts" having been recently replaced before sample preparation). It is likely that the milling was insufficient to reduce the grain size of all minerals. This effect has been previously reported

for platy minerals in other studies such as Wilson et al., (2009b) where large (~50□□m) phlogopite sheets (size confirmed by SEM imaging) remained after 10 minutes of milling in a McCrone mill. Alternative methods for reducing preferred orientation could be employed in future studies. For instance, the use of side-loading cavity mounts or spray drying of the samples (Hillier, 1999) could be employed to mitigate the effects of preferred orientation. However, it remains to be seen whether these more involved methods for sample preparation are practicable for the large numbers of samples that need to be analysed during carbon sequestration studies, and there are likely to be OH&S considerations that must be addressed before aerosolising serpentinite samples that commonly contain chrysotile.

Insert Figure 1 hereabouts

Insert Figure 2 hereabouts

Results and Discussion

Comparison of results from the three refinement methods

The results of using all three Rietveld refinement methods are shown in Tables 3, 4 & 5. These tables report the refined abundances for each phase, the estimated standard deviation (ESD, as reported in Topas V.5) and the difference between refined abundance and known abundance for each phase in every sample. Refined abundances obtained using the three methods are plotted against known abundances for each phase in Figure 3, where deviation from the ideal 1:1 trend indicates an over or underestimate. The absolute and relative errors on the refined values for all phases and all three methods are compared in Figure 4.

Insert Table 3 hereabouts

Insert Table 4 hereabouts

Insert Figure 3 hereabouts

This is a preprint, the final version is subject to change, of the American Mineralogist (MSA)
Cite as Authors (Year) Title. American Mineralogist, in press.
DOI: https://doi.org/10.2138/am-2018-6515

For the PONCKS and Pawley/internal standard methods, the largest source of error results from overestimation of serpentine mineral abundance (an average error of 4.6 wt% absolute and 6.0% relative) and the resulting systematic underestimation of the abundances of all minor phases. This can be seen in Figure 3e where the majority of data points lie above the 1:1 line, indicating the refined abundance is greater than the measured abundance. As a consequence of the overestimation of the serpentine abundance, the minor phases (all phases other than serpentine) tend to be underestimated, lying below the 1:1 line in most cases. This is not the case with the combined PONCKS-Pawley/internal standard method, which produced several instances of severe underestimates of serpentine abundance in the artificial tailings samples. This underestimation is likely occurring for the combined method because the abundance of serpentine and the abundance of amorphous material are being considered separately. Because these samples lack significant amorphous material (i.e., no amorphous phase was deliberately added), the amorphous content calculation represents more of a measure of the goodness of fit than an estimate of the amount of amorphous material in the samples. Asymmetry and peak broadening make fitting serpentine peaks difficult, making this the largest source of error when it comes to pattern fitting using a PONKCS phase. For samples with severely underestimated serpentine abundances, the unaccounted for intensity, which results in an overestimate of fluorite abundance, is then reported as 'amorphous' content.

Insert Table 4 hereabouts

Magnetite and hydromagnesite abundances tend to be underestimated using all three methods, and underestimates tend to be greater in samples with high abundances of these phases. The largest underestimate of magnetite abundance occurs for Artock1 when using the PONKCS method (3.6 wt% refined, 7.1 wt% weighed) and the largest underestimate of hydromagnesite occurs for Artock4 when using the PONKCS method (11.3 wt% refined, 15.0 wt% weighed). Preferred orientation issues could have led either to overestimations of refined abundances due

to uncharacteristically high peak heights or underestimations if preferred orientation corrections were used (as detailed above). However, the lack of appreciable preferred orientation displayed by hydromagnesite and magnetite makes either of these cases unlikely. The systematic underestimation of magnetite abundance may be related to microabsorption contrast given the relatively high linear absorption coefficient of magnetite compared to those of the silicate, hydroxide and carbonate minerals in the synthetic tailings samples. This underestimation may also stem in part from assumptions about particle size and shape that must be made in order to use of the Brindley correction for microabsorption contrast (e.g., Scarlett et al, 2002, Pederson et al., 2004). Underestimation of hydromagnesite abundance could be related to the asymmetric peak shapes observed for this phase. This asymmetry in the low angle peaks of hydromagnesite, which was modelled using a Thompson-Cox-Hastings pseudo-Voight profile, commonly occurs in naturally-occurring samples, such as this one, that have formed via decomposition of dypingite [$Mg_5(CO_3)_4(OH)_2 \cdot \sim 5H_2O$] to hydromagnesite (Wilson et al., 2010; Power et al., 2014). The systematic underestimation of these two minor phases could also be due to peak overlap with the serpentine minerals since the use of structureless pattern fitting methods tends to overestimate major phases, such as the lizardite and chrysotile that are modelled using this approach.

Pyroaurite and brucite show a different tendency to be overestimated at low abundances but then underestimated at higher abundances. The pyroaurite abundance for samples containing <4 wt% of this phase tended to be overestimated, whereas samples with >4 wt% pyroaurite produced underestimates of up to 6.3 wt% absolute (in sample Artrock8, which has a known pyroaurite abundance of 10.9 wt%). A similar, but less distinct trend occurs for brucite, with brucite abundances of <1 wt% tending to be overestimated and samples with >1 wt% tending to be underestimated. This likely occurs due to the difficulty in modelling severe preferred orientation for platy minerals such as pyroaurite and brucite. The March-Dollase preferred

orientation correction that was used may be overcompensating in samples with high abundances of platy minerals, leading to significantly lower refined abundances than those in which they are actually present. This switch from an overestimate to an underestimate is important to consider for carbon accounting purposes as it is more convoluted than if the phases were being consistently over- or underestimated.

The use of structureless pattern fitting is known to produce overestimates for those phases modelled using the approach, while producing systematic underestimates of other phases. Wilson et al. (2006) observed that these underestimates tend to be greatest for phases that are present at less than 5 wt% abundance. These observations have been reproduced by Wilson et al. (2009b) and Turvey et al. (2017). Underestimates on the abundances of minor phases are due to limitations in fitting anisotropic peaks using the fundamental parameters approach, difficulties in modelling preferred orientation (particularly for minerals that have a platy, fibrous or bladed morphology), and the tendency of refinements that include PONKCS models to incorrectly attribute the intensity of overlapping or adjacent reflections from other phases to the phase being modelled using the PONKCS method (Turvey et al., 2017; Wilson et al., 2009b).

Insert Figure 4 hereabouts

The relative error on refined mineral abundances is typically less than 50% for phases present at > 10 wt% abundance using all three methods (Figure 4). Relative error values tend to increase dramatically for phases present at < 2 wt% abundance. This increase in relative error at very low abundances has been seen in similar studies (Dipple et al., 2002 ; Raudsepp et al., 1999; Turvey et al., 2017; Wilson et al., 2006; Wilson et al., 2009b). However, even though the relative error increases substantially, because of the very low abundances of these phases, the corresponding absolute errors are still comparatively low. All three methods tend to give

relative errors in excess of 50% for low-abundance phases (<2 wt%) and, in several cases, the relative error values are in excess of 100% (Figure 4). The absolute error values for these phases, however, are still some of the lowest reported (Tables 3−5), and all are within 2 wt% of the actual known values (Figure 3 and 4). Thus, even though refined abundances for the minor phases such as the carbonate-bearing minerals, pyroaurite and hydromagnesite, suffer the largest relative error values at low abundances they are close to the actual known values.

Refinements using the PONKCS method produced greater values for the overall relative and absolute error compared with the Pawley/internal standard method with an average refinement bias (as defined by Omotoso et al., 2006) per sample of 10.3 wt%. Absolute error values for the minor (non-serpentine) phases gradually increased from <2 wt% at weighed abundances of <5 wt% to 2.0−6.6 wt% for phases at weighed abundances between 10 and 20 wt%. The relative error values are inversely proportional to the weighed abundances of a phase. Brucite was heavily underestimated with relative errors >50%, and the highest relative error value produced in the PONKCS refinements was for brucite: a 250% relative error was obtained for brucite in Artrock 5 (0.5 wt%), actual abundance 0.2 wt%.

The Pawley/internal standard method generally produced more accurate results than the PONKCS method, with an average refinement bias per sample of 6.7 wt%. Phases known to be present at <20 wt% abundance typically had absolute error values <2 wt% with the exception of the pyroaurite in samples Artrock6, 7 and 8, which contained the highest abundances of pyroaurite (4.9−9.8 wt%) and had absolute errors of 2.2−4.2 wt%. Although the relative error values for the Pawley/internal standard method are typically lower than those obtained using the PONKCS method, this approach produced the highest single relative error value in the study. Phases with <10 wt% abundance typically gave relative errors <50 %; however, a relative error of 367% for brucite abundance was recorded using this method, again for Artrock5, where a refined abundance of 0.9 wt% was obtained compared with the known value

of 0.2 wt%. However, this is not unexpected given that the abundance of brucite in this particular sample is close to the detection limit of ~0.1 wt% for this phase under the conditions used to collect XRD patterns during this study. Refined abundances for serpentine minerals using the Pawley/internal standard method were also more accurate than those obtained using the PONKCS method, with all serpentine abundances being within 5 wt% absolute and 6 % relative error. This is a minor improvement on results obtained using the PONKCS method in Turvey et al. (2017) (where serpentine was within 6 wt% absolute and 8% relative error) and using the Pawley/internal standard method in Wilson et al. (2006) and Wilson et al. (2009b) (where serpentine was within 5 wt% absolute and 11 % relative error).

The combined PONKCS Pawley/internal standard method produced results similar to those obtained using the PONKCS method, with an average refinement bias per sample of 12.9 wt%. Phases known to be present at <5 wt% abundance typically had absolute error values <2 wt% on refined abundances whereas phases present at between 5 and 15 wt% yielded absolute errors of between 2 and 6 wt%, similar to the results obtained using only the PONKCS method. Relative error values were typically <50% except for phases present at very low abundances (i.e., pyroaurite and brucite, where present at <2 wt%). Interestingly, the PONKCS Pawley/internal standard method produced relatively accurate results for phases present at very low abundances with relative errors all below 102% even for phases present at <2 wt% abundance (unlike the PONKCS and Pawley/internal standard methods which yielded extreme relative errors in some cases). One obvious weakness of the PONKCS Pawley/internal standard method is the poor accuracy of the refined abundances for the serpentine minerals, which is noticeably worse than using either the PONKCS or the Pawley/internal standard method alone. Absolute error values of 0.2−15.6 wt% were reported for serpentine when using the combined method (up to 19.3 % relative error), greater than errors of 1.0−11.6 wt% for the PONKCS method (up to 14.7 % relative error) and significantly greater than errors obtained when

estimating the serpentine abundance using the Pawley/internal standard method (0.0−4.7 wt%, up to 6.6% relative error).

The ESD values reported in Tables 3−5, give an indication of the precision with which each mineral phase is measured using the three refinement methods that were tested. Refined abundances for pyroaurite, magnetite and brucite have similar ESD values of 0.1−0.3 wt%. Hydromagnesite and serpentine abundances have larger ESD values: 0.3−1.0 wt% for hydromagnesite and 0.5−3.0 at% for serpentine. The three different refinement methods used in this study do not give significantly different ESD values for pyroaurite, magnetite and brucite for a given. However, which refinement method is used does appear to affect ESD values for hydromagnesite and serpentine, with the Pawley/internal standard method having the largest ESD values for hydromagnesite (0.4−1.0 wt%) but the lowest values for serpentine (0.5−1.1 wt%). For pyroaurite, magnetite and serpentine, the values for refined mineral abundance are significantly larger than the corresponding ESD values. The ESD values for these three phases are typically smaller in magnitude than the over- and underestimates between modelled abundance and known abundance observed for each mineral. However the ESD values for brucite and hydromagnesite are of a similar to the differences observed between the refined and known abundances. This indicates that the errors on refined abundances for these two minerals may largely be driven by the precision of the measurements rather than systematic over- or underestimation.

Estimates of carbon sequestration and carbonation potential

Insert Table 6.

Insert Figure 5.

Table 6 and Figure 5 show estimates of the carbon sequestered and the carbonation potential of each of the artificial tailings samples according to their weighed and refined abundances of

carbonate minerals and brucite, respectively. The carbon sequestered in the tailings samples is reported here as the amount of CO_2 contained in the hydromagnesite and pyroaurite in a sample, and the carbonation potential is an estimate of the amount of CO_2 that could be sequestered assuming brucite is altered to either pyroaurite or hydromagnesite. Hydromagnesite and pyroaurite have been reported to sequester atmospheric CO_2 in previous studies of carbonation reactions in mine tailings (e.g., Oskierski et al., 2013; Wilson et al., 2014), they represent the amount of atmospheric CO_2 that has already been sequestered in a tailings sample. Brucite is reported as the primary Mg source for passive carbonation of mine tailings at many sites (e.g., Oskierski et al., 2013; Wilson et al., 2014), where it can be replaced by hydromagnesite, dypingite, nesquehonite ($MgCO_3 \cdot 3H_2O$) or pyroaurite (Harrison et al., 2015; Harrison et al., 2013; Oskierski et al., 2013; Wilson et al., 2010; Wilson et al., 2014), where dypingite and nesquehonite are more likely to form and persist in colder climates than that of New South Wales. Thus the brucite abundance in tailings samples can be considered analogous to the amount of future carbonation potential possible for the sample (Wilson et al., 2014). Whether brucite is altered to hydromagnesite or pyroaurite at Woodsreef will largely determine the amount of CO_2 that could be sequestered at this and other mine sites. Assuming that brucite can produce either a high−C phase (hydromagnesite, which is 37.6 % CO_2 by weight) or a low−C phase (pyroaurite, which is 6.7 % CO_2 by weight) provides an upper and lower estimate for the carbonation potential of brucite and both scenarios are considered in Table 6 and Figure 5. Figure 5 compares (1) the amount of CO_2 currently sequestered in each of the tailings samples (calculated using the abundances of pyroaurite and hydromagnesite and their stoichiometric CO_2 content) and (2) the potential amount of future carbon sequestration (calculated using the abundance of brucite and the stoichiometric CO_2 content of hydromagnesite or pyroaurite) obtained using the three Rietveld refinement methods. The results in Figure 5 demonstrate that all three refinement methods result in systematic

underestimates of the known extents of carbon sequestration and carbonation potential of the artificial tailings samples, except for Artrock1 and Artrock5. Of the three methods, the Pawley/internal standard produced the most consistently accurate results, giving the closest estimate to the known values for carbon content of the artificial tailings samples, with an average absolute error of 0.6 g CO_2 (25.4 % relative error). The PONKCS and Pawley/internal standard methods are typically quite similar in terms of the accuracy with which they estimate C content; however, in the case of Artrock4 and Artrock8, the Pawley/internal standard method offers significantly better results (8.0 % relative error compared with 22.9 % error for Artrock4 and 21.5 % relative error compared with 63.0 % error for Artrock8). The combined PONKCS Pawley/internal standard method consistently produced the least accurate results, with an average absolute error of 1.2 g of CO_2 per sample, compared with 0.9 g of CO_2 for the PONKCS method and 0.6 g of CO_2 for the Pawley/internal standard method (relative errors of 34.4 %, 36.2 % and 25.4 % respectively). However, the PONKCS Pawley/internal standard method did yield more accurate results for wt% CO_2 content of Artrock1 and Artrock5, whereas the other two methods yielded significant overestimates for the known amount of sequestered CO_2.

Hydromagnesite abundance is the greater contributor to the carbon sequestration and carbonation potential of most of the tailings samples owing to its high stoichiometric CO_2 content. The results in Figure 5 indicate that the large errors that occur in estimating the abundances of carbonate minerals in the synthetic tailings have a significant effect on estimates of carbon sequestration and carbonation potential. These errors result in consistent underestimation of the amount of CO_2 sequestered in the samples as well as their potential to sequester additional CO_2 by carbonation of unreacted brucite. This is particularly noticeable when considering the mass of CO_2 sequestered in pyroaurite and the carbonation potential of brucite, both of which minerals suffer from severe preferred orientation. At high abundances

of pyroaurite and brucite, the use of the PONKCS and the PONKCS-Pawley/internal standard methods in particular leads to significant underestimates of the abundances of these minerals (as seen in Figure 3). Underestimates of the abundances of pyroaurite and brucite result in a corresponding underestimation of the amount of CO_2 sequestered in the pyroaurite and the carbonation potential of brucite in a given sample. This is most apparent for Artock8, where the high pyroaurite abundance (10.9 wt%) was underestimated using all three methods (i.e., underestimates of 5.6 wt% using the Pawley/internal standard method, 4.3 wt% using the PONKCS method and 4.4 wt% using the combined PONKCS-Pawley/internal standard method), leading to a large discrepancy between the amount of CO_2 sequestered in pyroaurite (0.72 g CO_2) and the amount that is estimated using the various refinement methods (estimated at 0.37 g CO_2 using the Pawley/internal standard method, 0.29 g CO_2 using the PONKCS method and 0.29 g CO_2 using the combined PONKCS-Pawley/internal standard method).

The use of all three refinement methods tends to result in underestimates for all minor phases, including carbonate-bearing phases. These refinement methods also cannot be used to quantify the amount of amorphous carbonate in a sample independently from other amorphous phases, thus it is likely that the use of Rietveld refinement methods for carbon accounting leads to underestimates of the amount of CO_2 sequestered in a sample. Thus carbon accounting XRD likely provides a conservative estimate of the amount of CO_2 sequestered in mine tailings. Understanding the advantages and disadvantages of XRD-based methods for carbon accounting allows for improved comparison with other methods. Elemental C analysis can be used to provide a more accurate and direct estimate of the amount of CO_2 sequestered in a sample, but it cannot be used to differentiate between atmospheric carbon and carbon from other sources nor can it quantify the relative amounts of atmospheric and bedrock carbon in specific minerals. Thermal decomposition of brucite can provide a very accurate estimate of the amount of this highly reactive mineral in a sample (Assima et al., 2013b), making it

appropriate for estimating the carbonation potential of a sample; however, complementary methods should be used to estimate the amount of CO_2 sequestration that has already occurred.

Method comparison

The PONKCS method has several advantages over other Rietveld refinement methods for dealing with structurally disordered phases such as serpentine minerals. It does not require (1) the addition of an internal standard to the samples; (2) experimental reference patterns for all minerals in a given sample or (3) specialized and labour-intensive preparation of specimens (Scarlett and Madsen, 2006; Turvey et al., 2017). However, these advantages must be weighed against the superior accuracy obtained using the Pawley/internal standard method. The accuracy with which the abundances of carbonate-bearing minerals can be estimated is the most important factor when using X-ray diffraction to estimate the amount of CO_2 sequestered in tailings or similar materials. Accurate measurements of the abundances of brucite, in particular, and also of serpentine minerals are most important for estimating future carbonation potential. The Pawley/internal standard method produces more accurate estimates for pyroaurite and hydromagnesite abundances in the artificial tailings samples (Table 4, Figure 3). The absolute error values for the hydromagnesite abundances obtained using the Pawley/internal standard method were typically <1 wt% for abundances of 0.9−13.5 wt%. This also resulted in relative error values of <20%. Estimates of pyroaurite abundance were not as accurate, with absolute errors of 2 wt% being typical for samples with <5 wt% pyroaurite and absolute errors of up to 4 wt% for abundances between 5 and 10 wt%. Therefore, we recommended that an internal standard be used with structureless pattern fitting of XRD data in order to more accurately estimate CO_2 fixation in mine tailings. However, the PONKCS method has the distinct advantage that it can be applied in the field alongside portable XRD instruments, where quickly generating usable data is more important than maximising the accuracy of the analyses (Turvey et al., 2017).

This is a preprint, the final version is subject to change, of the American Mineralogist (MSA)
Cite as Authors (Year) Title. American Mineralogist, in press.
DOI: https://doi.org/10.2138/am-2018-6515

Although the combined PONKCS-Pawley/internal standard method produced less accurate results than either the PONKCS or Pawley/internal standard methods, it does offer a feature not permitted by either of the other methods: the possibility to independently quantify multiple disordered phases using PONKCS models while measuring amorphous material using an internal standard, without have to calibrate a PONKCS phase for each amorphous component. Use of this combined method could make it possible to quantify the various disordered and amorphous phases in a sample without necessarily having to calibrate PONKCS models for all of them. In samples that do not contain detectable levels of amorphous material, such as the artificial tailings samples that were studied here, the refined abundance for 'amorphous' content could also potentially be used as a test of the 'goodness of fit' for refinements that include PONKCS phases, because unaccounted for intensity will contribute to the refined value for 'amorphous' content. It is important to consider that amorphous material is typically not visible (as broad peaks) in XRD patterns when present at abundances below 20 or 30 wt%. As such, this method should only be applied when amorphous material is known to be present in a sample, for instance should it be present at a sufficiently high abundance to be detectable from an XRD pattern. It should not be used in those cases where amorphous content does not produce any detectable peaks in an XRD pattern. This method could also potentially be used to distinguish between various disordered phases such as the polymorphs of serpentine, lizardite and chrysotile, which are difficult to discriminate in XRD patterns of multiphase materials. It was found that the refined values for 'amorphous' content for Artrock1−4 were relatively low <4 wt% whereas those for Artrock5−8 where significantly higher, 14−18 wt%. It should be noted that a physically impossible refined value of -5.9 wt% 'amorphous' content was obtained for Artrock1 as an artefact of refined fluorite abundance being less that the known value of 10 wt%. The difference in the estimated abundance of 'amorphous' content for the two groups of Artrock samples can be explained by the use of two different serpentine minerals to make

Artrock samples, with a sample of picrolite (chrysotile) being used for Artrock1−4 and a sample of lizardite being used in Artrock5−8. The two different mineral standards may have differing levels of amorphous material which could lead to the differences in refined 'amorphous' content. However, it is more likely that the use of a single chrysotile PONKCS model for evaluating the serpentine content in all of the samples, rather than chrysotile for Artrocks1−4 and lizardite for Artrocks5−8, resulted in this inaccurate estimate in samples that do not contain appreciable amorphous material but do contain a different polymorph of serpentine (i.e., lizardite). While the combined method does offer a way to separately quantify multiple disordered or amorphous phases and may provide an estimate of the goodness of fit, care must be used when applying it as use of the method can give rise to non-physical values for amorphous content in cases where there is no or very little amorphous material and the refined abundance for the fluorite spike (before normalization using Eq.2) is lower than the actual abundance of the internal standard. In this scenario a negative abundance for amorphous content will be reported (this occurred for Artrock1). As such, it is important to carefully apply the combined PONKCS Pawley/internal standard method to avoid unphysical results and overestimates of amorphous material.

Implications

When performing quantitative phase analysis of samples that include structurally disordered phases, such as serpentine minerals, it is important to choose a Rietveld refinement approach that gives the most accurate possible results. We have found that of the three methods tested here, the most accurate results were produced by the Pawley/internal standard method, justifying the addition of an internal standard to each sample. The more flexible PONKCS method is more suitable for obtaining geochemically useful quantitative results quickly in the course of fieldwork with a portable XRD (Turvey et al., 2017). But if a more robust accounting of carbon fixation in tailings material is required, an internal standard should be added to each

sample. The combined PONKCS-Pawley/internal standard method, although less accurate than either the Pawley/internal standard method or the PONKCS method, could potentially be of use when analysing samples such as tailing material from ultramafic mines that may contain amorphous carbonate and silica phases. The ability to independently quantify multiple disordered phases could be necessary when investigating carbon sequestration and carbonation potential because carbonation reaction can produce amorphous hydrated carbonated phases as well as well-ordered minerals such as pyroaurite, and hydromagnesite (e.g., Harrison et al., 2015).

By optimizing and assessing the accuracy of both the PONKCS and Pawley/internal standard methods, we are laying the groundwork for further crystallographic carbon accounting at Woodsreef and similar mine sites. Previous XRD studies at Woodsreef used small sample sets to estimate the amount of CO_2 stored in mine tailings: Oskierski et al. (2013) investigated eight samples from the tailings at Woodsreef and Turvey et al. (2017) used another six. A large-scale XRD study could be used to refine previous estimates for CO_2 sequestration at Woodsreef, which vary from 1400 t to 70,000 t of CO_2 sequestered in the tailings pile (Oskierski et al., 2013). Such a study should use samples from many locations and from different depths below the surface of the tailings storage facility at Woodsreef to improve the accuracy of estimations of CO_2 sequestration at this locality. This work has determined the optimal Rietveld refinement strategy for tailings from the Woodsreef mine and samples from mineralogically similar mines. It has also resulted in a systematic analysis of which mineral abundances are under- and overestimated during Rietveld refinement, making it possible to predict that minor phases including carbonate-bearing phases will likely be underestimated using XRD data for carbon accounting.

With a firm understanding of the limitations and advantages of the various methods and their application to carbon accounting, quantitative XRD can be used more effectively to quantify

carbon sequestration within ultramafic tailings and natural landscapes. Although the use of Rietveld-based methods tends to underestimate minor phases, and thus is likely to result in underestimates of the current carbon sequestration and future carbonation potential of a mine site, these methods can be used to determine an effective baseline of the amount of CO_2 that is being sequestered in mineralogically complex tailings. Crystallographic carbon accounting methods are also unlikely to result in gross overestimates of CO_2 sequestration in minerals and the carbonation potential of mineral wastes and rocks, both which are likely to become important in situations where regulatory monitoring of carbon sequestration is introduced.

Acknowledgements

We would like to thank Jenine McCutcheon and Gordon Southam for their invaluable assistance in the field. We would like to acknowledge the financial assistance of Carbon Management Canada and the New South Wales Department of Industry. We would also like to thank Kate Maddison, Nick Staheyeff, Catherine Karpiel and Brad Mullard at the NSW Department of Industry for granting us access to the field site and for their support of our work at Woodsreef. We thank Ben Grguric for providing a sample of iowaite from the Mount Keith nickel mine. Work by C.C. Turvey and J.L. Hamilton was supported by Australian Postgraduate Awards. We are grateful to David Bish and an anonymous reviewer for their constructive advice that has helped us to improve our work. Our thanks go to Warren Huff for editorial handling of this manuscript.

References

Akao, M., and Iwai, S. (1977) The hydrogen bonding of hydromagnesite. Acta Crystallographica Section B, 33 (4), 1273-1275.

Alexander, L., and Klug, H.P. (1948) Basic aspects of X-ray absorption in quantitative diffraction analysis of powder mixtures. Analytical Chemistry, 20 (10), 886-889.

Assima, G.P., Larachi, F., Beaudoin, G., and Molson, J. (2013a) Dynamics of carbon dioxide uptake in chrysotile mining residues – Effect of mineralogy and liquid saturation. International Journal of Greenhouse Gas Control, 12, 124-135.

Assima, G.P., Larachi, F., Molson, J., and Beaudoin, G. (2013b) Accurate and direct quantification of native brucite in serpentine ores—New methodology and implications for CO_2 sequestration by mining residues. Thermochimica Acta, 566, 281-291.

Assima, G.P., Larachi, F., Molson, J., and Beaudoin, G. (2014a) Emulation of ambient carbon dioxide diffusion and carbonation within nickel mining residues. Minerals Engineering, 59, 39-44.

Assima, G.P., Larachi, F., Molson, J., and Beaudoin, G. (2014b) New tools for stimulating dissolution and carbonation of ultramafic mining residues. The Canadian Journal of Chemical Engineering, 92 (12), 2029-2038.

Assima, P.G., Larachi, F., Beaudoin, G., and Molson, J.W. (2012) CO_2 sequestration in chrysotile mining residues - Implication of watering and passivation under environmental conditions. Industrial & Engineering Chemistry Research, 51 (26), 8726-8734.

Bea, S.A., Wilson, S.A., Mayer, K.U., Dipple, G.M., Power, I.M., and Gamazo, P. (2012) Reactive transport modeling of natural carbon sequestration in ultramafic mine tailings. Vadose Zone Journal, 11(2).

Beaudoin, G., Nowamooz, A., Assima, G.P., Lechat, K., Gras, A., Entezari, A., Kandji, E.H.B., Awoh, A.-S., Horswill, M., Turcotte, S., Larachi, F., Dupuis, C., Molson, J., Lemieux, J.-M., Maldague, X., Plante, B., Bussière, B., Constantin, M., Duchesne, J., Therrien, R., and Fortier, R. (2017) Passive mineral carbonation of Mg-rich mine wastes by atmospheric CO_2. Energy Procedia, 114, 6083-6086.

Beinlich, A., and Austrheim, H. (2012) In situ sequestration of atmospheric CO_2 at low temperature and surface cracking of serpentinized peridotite in mine shafts. Chemical Geology, 332–333, 32-44.

Berner, R.A. (1990) Atmospheric carbon dioxide levels over phanerozoic time. Science, 249 (4975), 1382-1386.

Bish, D.L. (1980) Anion-exchange in takovite: applications to other hydrotalcite minerals. Bulletin Mineralogie, 103, 170-175.

Bish, D.L., and Howard, S.A. (1988) Quantitative phase analysis using the Rietveld method. Journal of Applied Crystallography, 21(2), 86-91.

Bobicki, E.R., Liu, Q., Xu, Z., and Zeng, H. (2012) Carbon capture and storage using alkaline industrial wastes. Progress in Energy and Combustion Science, 38(2), 302-320.

Brindley, G.W. (1945) XLV. The effect of grain or particle size on x-ray reflections from mixed powders and alloys, considered in relation to the quantitative determination of crystalline substances by x-ray methods. Philosophical Magazine Series 7, 36(256), 347-369.

Catti, M., Ferraris, G., Hull, S., and Pavese, A. (1995) Static compression and H disorder in brucite, $Mg(OH)_2$, to 11 Gpa: a powder neutron diffraction study. Physics and Chemistry of Minerals, 22, 200-206.

Chang, E.E., Chen, C.H., Chen, Y.H., Pan, S.Y., and Chiang, P.C. (2011) Performance evaluation for carbonation of steel-making slags in a slurry reactor. J Hazard Mater, 186(1), 558-64.

Cheary, R.W., and Coelho, A. (1992) A fundamental parameters approach to X-ray line-profile fitting. Journal of Applied Crystallography, 25(2), 109-121.

Chung, F.H. (1974) Quantitative interpretation of X-ray diffraction patterns of mixtures 1. Matrix-flushing method for quantitative multicomponent analysis. Journal of Applied Crystallography, 7(6).

Cleugh, H., Smith, M.S., Battaglia, M., and Graham, P. (2011) Climate change science and solutions for Australia. CSIRO Publishing, 150 Oxford Street Collingwood VIC Australia.

Dipple, G.M., Raudsepp, M., and Gordon, T.M. (2002) Assaying wollastonite in skarn. In Industrial Minerals in Canada, Canadian Istitute of Mining Metallurgy and Petroleum Special Volume, 53, 303-312.

Dollase, W. (1986) Correction of intensities for preferred orientation in powder diffractometry: application of the March model. Journal of Applied Crystallography, 19(4), 267-272.

Falini, G., Foresti, E., Gazzano, M., Gualtieri, A.F., Leoni, M., Lesci, I.G., and Roveri, N. (2004) Tubular-shaped stoichiometric chrysotile nanocrystals. Chemistry, 10(12), 3043-3049.

Gualtieri, A.F. (2000) Accuracy of XRPD QPA using the combined Rietveld-RIR method. Journal of Applied Crystallography, 33(2), 267-278.

Hamilton, J.L., Wilson, S.A., Morgan, B., Turvey, C.C., Paterson, D.J., Jowitt, S., McCutcheon, J., and Southam, C. (2018) Fate of transition metals during passive carbonation of ultramafic mine tailings via air capture with potentials for metal resource recovery. International Journal of Greenhouse Gas Control, In Press.

Hamilton, J.L., Wilson, S.A., Morgan, B., Turvey, C.C., Paterson, D.J., MacRae, C., McCutcheon, J., and Southam, G. (2016) Nesquehonite sequesters transition metals and CO_2 during accelerated carbon mineralisation. International Journal of Greenhouse Gas Control, 55, 73-81.

Harrison, A.L., Dipple, G.M., Power, I.M., and Mayer, K.U. (2015) Influence of surface passivation and water content on mineral reactions in unsaturated porous media: Implications for brucite carbonation and CO2 sequestration. Geochimica et Cosmochimica Acta, 148, 477-495.

Harrison, A.L., Power, I.M., and Dipple, G.M. (2013) Accelerated carbonation of brucite in mine tailings for carbon sequestration. Environmental Science and Technology, 47(1), 126-134.

Hill, R.J., and Howard, C.J. (1987) Quantitative phase analysis from neutron powder diffraction data using the Rietveld method. Journal of Applied Crystallography, 20(6), 467-474.

Hillier, S. (1999) Use of an air brush to spray dry samples for X-ray powder diffraction. Clay Minerals, 34, 127–135.

Hitch, M., Ballantyne, S.M., and Hindle, S.R. (2010) Revaluing mine waste rock for carbon capture and storage. International Journal of Mining, Reclamation and Environment, 24(1), 64-79.

Houghton, J.T., Ding, Y., Griggs, D.J., Noguer, M., van der Linden, P.J., Dai, X., Maskell, K., and Johnson, C.A. (2001) Climate Change 2001: The scientific basis: Contribution of Working Group 1 to the third assessment report of the Intergovernmental Panel on Climate Change. Cambridge University Press, U.K.

IPCC. (2005) IPCC special report on carbon dioxide capture and storage. In O.D. Bert Metz, Heleen de Coninck, Manuela Loos, Leo Meyer, Ed, p. 442. Cambridge University Press, 40 West 20th Street, New York, NY 10011–4211, USA.

IPCC. (2013) Climate Change 2013: The physical science basis. In IPCC, Ed. IPCC Working Group 1.

IPCC. (2014) Climate Change 2014: Mitigation of climate change. In IPCC, Ed. IPCC Working Group 3.

Kump, L.R., Brantley, S.L., and Arthur, M.A. (2000) Chemical weathering, atmospheric CO_2 and climate. Annual Review of Earth and Planetary Sciences, 28, 611-67.

Lackner, K.S. (2002) Carbonate chemistry for sequestering fossil carbon. Annual review of energy and the environment, 27(1), 193-232.

Lackner, K.S. (2003) A guide to CO_2 sequestration. Science, 300, 1677-1678.

Lackner, K.S., Wendt, C.H., Butt, D.P., Joyce Jr, E.L., and Sharp, D.H. (1995) Carbon dioxide disposal in carbonate minerals. Energy, 20(11), 1153-1170.

Laughton, C.A., and Green, N. (2002) Woodsreef magnesium project: An example of sustainable mineral waste processing from mined ore and its utilisation to produce refined metal products. Green Processing 2002. New South Wales Department of Mineral Resources, St Leonards, N.S.W., Australia, Cairns, QLD.

Lechat, K., Lemieux, J.M., Molson, J.W., Beaudoin, G., and Hebert, R. (2016) Field evidence of CO_2 sequestration by mineral carbonation in ultramafic milling wastes, Thetford Mines, Canada. International Journal of Greenhouse Gas Control, 47, 110-121.

Leung, D.Y.C., Caramanna, G., and Maroto-Valer, M.M. (2014) An overview of current status of carbon dioxide capture and storage technologies. Renewable and Sustainable Energy Reviews, 39, 426-443.

Leventouri, T. (1997) A new method for measuring the degree of preferred orientation in bulk textured YBa2Cu3Ox. Physica C: Superconductivity, 277(1–2), 82-86.

March, A. (1932) Mathematische theorie der regelung nach der korn gestalt bei affiner deformation. Zeitschrift für Kristallographie 81, 285-297.

McCutcheon, J., Dipple, G.M., Wilson, S.A., and Southam, G. (2015) Production of magnesium-rich solutions by acid leaching of chrysotile: A precursor to field-scale

deployment of microbially enabled carbonate mineral precipitation. Chemical Geology, 413, 119-131.

McCutcheon, J., Turvey, C.C., Wilson, S.A., Hamilton, J.L., and Southam, G. (2017) Mine site deployment of microbial carbonation for the stabilization of asbestos mine tailings. Geochimica et Cosmochimica Acta, Accepted in Press.

McCutcheon, J., Wilson, S.A., and Southam, G. (2016) Microbially accelerated carbonate mineral precipitation as a strategy for in situ carbon sequestration and rehabilitation of asbestos mine sites. Environmental Science & Technology, 50(3), 1419-1427.

Mellini, M., and Viti, C. (1994) Crystal structure of lizardite-1T from Elba, Italy. American Mineralogist, 79(11-12), 1194-1198.

Merril, R.J., Butt, B.C., Forrest, V.C., Purdon, G., and Bramley-Moore, R.A. (1980) Asbestos production at Chrysotile Corporation of Australia Pty. Limited, Barraba, N.S.W. In J.T. Woodcock, Ed. Mining and metallurgical practices in Australasia, 10, p. 669-673. The Australasian Institute of Mining and Metallurgy, Clunies Ross House, 191 Royal Parade, Parkville, Victoria, Australia 3052.

Millar, R.J., Fuglestvedt, J.S., Friedlingstein, P., Rogelj, J., Grubb, M.J., Matthews, H.D., Skeie, R.B., Forster, P.M., Frame, D.J., and Allen, M.J. (2017) Emission budgets and pathways consistent with limiting warming to 1.5°C. Nature Geoscience, 10, 741-748.

Miyata, S. (1983) Anion-exchange properties of hydrotalcite-like compounds. Clays and Clay Minerals, 31(4), 305-311.

Oelkers, E.H., Gislason, S.R., and Matter, J. (2008) Mineral carbonation of CO_2. Elements, 4, 333-337.

Olowe, A. (1995) Crystal structures of pyroaurite and sjoegrenite. Advances in X-ray Analysis, 38, 749-755.

Omotoso, O., McCarty, D.K., Hillier, S., and Kleeberg, R. (2006) Some successful approaches to quantitative mineral analysis as revealed by the 3rd Reynolds Cup contest. Clays and Clay Minerals, 54(6), 748-760.

Oskierski, H.C., Dlugogorski, B.Z., and Jacobsen, G. (2013) Sequestration of atmospheric CO_2 in chrysotile mine tailings of the Woodsreef asbestos mine, Australia: quantitative mineralogy, isotopic fingerprinting and carbonation rates. Chemical Geology.

Pacala, S., and Socolow, R. (2004) Stabilization wedges: Solving the climate problem for the next 50 years with current technologies. Science, 305.

Pawley, G. (1981) Unit-cell refinement from powder diffraction scans. Journal of Applied Crystallography, 14(6), 357-361.

Pederson, B.M., Schaible, K.J., and Winburn, R.S. (2004) Minimization of errors due to microabsorption or absorption contrast. Advances in X-ray Analysis, 47, 200-205.

Power, I.M., Harrison, A.L., Dipple, G.M., Wilson, S.A., Kelemen, P.B., Hitch, M., and Southam, G. (2013a) Carbon mineralization: From natural analogues to engineered systems. Reviews in Mineralogy & Geochemistry, 77, 305-360.

Power, I.M., Wilson, S.A., and Dipple, G.M. (2013b) Serpentinite carbonation for CO_2 sequestration. Elements, 9, 115-121.

Power, I.M., Wilson, S.A., Harrison, A.L., Dipple, G.M., McCutcheon, J., Southam, G., and Kenward, P.A. (2014) A depositional model for hydromagnesite–magnesite playas near Atlin, British Columbia, Canada. Sedimentology, 61(6), 1701-1733.

Pronost, J., Beaudoin, G., Lemieux, J.M., Hebert, R., Constantin, M., Marcouiller, S., Klein, M., Duchesne, J., Molson, J.W., Larachi, F., and Maldague, X. (2012) CO_2-depleted warm air venting from chrysotile milling waste (Thetford Mines, Canada): Evidence for in-situ carbon capture from the atmosphere. Geology, 40(3), 275-278.

Pronost, J., Beaudoin, G., Tremblay, J., Larachi, F., Duchesne, J., Hebert, R., and Constantin, M. (2011) Carbon sequestration kinetic and storage capacity of ultramafic mining waste. Environ Sci Technol, 45(21), 9413-20.

Raudsepp, M., Pani, E., and Dipple, G.M. (1999) Measuring mineral abundance in skarn. I. The Rietveld method using X-ray powder-diffraction data. The Canadian Mineralogist, 13 (1-15).

Rietveld, H. (1969) A profile refinement method for nuclear and magnetic structures. Journal of Applied Crystallography, 2(2), 65-71.

Rinaudo, C., Gastaldi, D., and Bulluso, E. (2003) Characterization of chrysotile, antigorite and lizardite by FT-Raman spectroscopy. Canadian Mineralogist, 41, 883−890.

Scarlett, N.V.Y., and Madsen, I.C. (2006) Quantification of phases with partial or no known crystal structures. Powder Diffraction, 21(4), 278-284.

Scarlett, N.V.Y., Madsen, I.C., Cranswick, L.M.D., Lwin, T., Groleau, E., Stephenson, G., Aylmore, M., and Agron-Olshina, N. (2002) Outcomes of the International Union of Crystallography Commission on Powder Diffraction Round Robin on Quantitative Phase Analysis: samples 2, 3, 4, synthetic bauxite, natural granodiorite and pharmaceuticals. Journal of Applied Crystallography, 35, 383-400.

Seifritz, W. (1990) CO_2 disposal by means of silicates. Nature, 345.

Stephens, P.W. (1999) Phenomenological model of anisotropic peak broadening in powder diffraction. Journal of Applied Crystallography, 32, 281-289.

Tsukimura, K., Sasaki, S., and Kimizuka, N. (1997) Cation distributions in nickel ferrites. Japanese Journal of Applied Physics, 36(6R), 3609.

Turvey, C.C., Wilson, S.A., Hamilton, J.L., and Southam, G. (2017) Field-based accounting of CO_2 sequestration in ultramafic mine wastes using portable X-ray diffraction. American Mineralogist.

Von Dreele, R.B. (1997) Quantitative texture analysis by Rietveld refinement. Journal of Applied Crystallography, 30(4), 517-525.

Whitfield, P.S. (2008) Spherical harmonics preferential orientation corrections and structure solution from powder diffraction data - a possible avenue of last resort. Journal of Applied Crystallography, 42, 134-136.

Wicks, F.J. (2000) Status of the reference X-ray powder-diffraction patterns for the serpentine minerals in the PDF database – 1997. Powder Diffraction, 15, 42–50.

Wicks, F.J., and Whittaker, E.J.W. (1975) A reappraisal of the structures of the serpentinte minerals Canadian Mineralogist, 13, 227-243.

Wilson, S.A., Harrison, A.L., Dipple, G.M., Power, I.M., Barker, S.L.L., Mayer, K.U., Fallon, S.J., Raudsepp, M., and Southam, G. (2014) Offsetting of CO2 emissions by air capture in mine tailings at the Mount Keith Nickel mine, Western Australia: Rates, controls and propects for carbon neutral mining. International Journal of Greenhouse Gas Control, 25, 121-140.

Wilson, S.A., Barker, S.L.L., Dipple, G.M., Atudorei, V. (2010) Isotopic disequilibrium during uptake of atmospheric CO2 into mine process waters: implications for CO2 sequestration. Environmental Science & Technology, 44, 9522–9529.

Wilson, S.A., Dipple, G.M., Power, I.M., Thom, J.M., Anderson, R.G., Raudsepp, M., Gabites, J.E., and Southham, G. (2009a) Carbon dioxide fixation within mine wastes of ultramafic-hosted ore deposits: Examples from the Clinton Creek and Cassiar chrysotile deposits, Canada. Economic geology, 104, 95–112.

Wilson, S.A., Raudsepp, M., and Dipple, G.M. (2009b) Quantifying carbon fixation in trace minerals from processed kimberlite; a comparative study of quantitative methods using X-ray powder diffraction data with applications to the Diavik diamond mine, Northwest Territories, Canada. Applied Geochemistry, 24(12), 2312-2331.

Wilson, S.A., Raudsepp, M., and Dipple, G.M. (2006) Verifying and quantifying carbon fixation in minerals from serpentine-rich mine tailings using the Rietveld method with X-ray powder diffraction data. American Mineralogist, 91(8-9), 1331-1341.

This is a preprint, the final version is subject to change, of the American Mineralogist (MSA)
Cite as Authors (Year) Title. American Mineralogist, in press.
DOI: https://doi.org/10.2138/am-2018-6515

Tables

Table 1. Weighed composition of artificial tailings samples

		Artrock1	Artrock2	Artrock3	Artrock4	Artrock5	Artrock6	Artrock7	Artrock8
Pyroaurite	(wt%)	1.9	3.2	3.2	3.3	1.3	5.4	7.6	10.9
Magnetite	(wt%)	7.1	5.0	5.0	5.0	5.0	5.0	5.1	3.0
Brucite	(wt%)	1.1	1.8	1.8	1.8	0.2	1.1	1.5	2.2
Hydromagnesite	(wt%)	1.0	5.0	10	15	3.6	5.0	5.0	5.0
Serpentine	(wt%)	88.9	85	80	74.9	89.9	83.5	80.8	78.9
Total[a]	(wt%)	100.0	100.0	100.0	100.0	100.0	100.0	100.0	100.0

[a] Total mass of each sample was 100 g.

Table 2. Sources of crystal-structure data for Rietveld refinement

Mineral	Source
Pyroaurite	Olowe (1995)
Magnetite	Tsukimura et al. (1997)
Brucite	Catti et al. (1995)
Hydromagnesite	Akao and Iwai (1977)
Chrysotile	Falini et al. (2004)
Lizardite	Mellini and Viti (1994)

This is a preprint, the final version is subject to change, of the American Mineralogist (MSA)
Cite as Authors (Year) Title. American Mineralogist, in press.
DOI: https://doi.org/10.2138/am-2018-6515

Table 3. Refinement results for PONKCS method

Sample	Abundance	Pyro-aurite	Magn-etite	Brucite	Hydrom-agnesite	Serpentine	Total	R_{wp} [a]	χ^2 [b]	d [c]	Total bias [d]
	weighed (%)	1.9	7.1	1.1	1.0	88.9	100.0				
Artrock1	refined (ESD[e])	2.7 (0.2)	3.6 (0.1)	2.6 (0.1)	1.0 (0.4)	90.1 (1.5)	100.0	15.4	4.4	0.2	
	difference	+0.8	-3.5	+1.5	+0.0	+1.2					7.0
	weighed (%)	3.2	5.0	1.8	5.0	85	100.0				
Artrock2	refined (ESD[e])	4.3 (0.1)	3 (0.1)	1.1 (0.1)	4.4 (0.5)	87.1 (1.4)	100.0	11.9	3.5	0.2	
	difference	+1.1	-2.0	-0.7	-0.6	+2.1					6.5
	weighed (%)	3.2	5.0	1.8	10.0	80	100.0				
Artrock3	refined (ESD[e])	4.4 (0.1)	2.6 (0.1)	1.3 (0.1)	8 (0.3)	83.6 (1.0)	100.0	11.2	3.8	0.2	
	difference	+1.2	-2.4	-0.5	-2.0	+3.6					9.7
	weighed (%)	3.3	5.0	1.8	15.0	74.9	100.0				
Artrock4	refined (ESD[e])	4.7 (0.1)	3 (0.1)	1.3 (0.1)	11.3 (0.4)	79.7 (1.0)	100.0	11.1	3.6	0.2	
	difference	+1.4	-2.0	-0.5	-3.7	+4.8					12.3
	weighed (%)	1.3	5.0	0.2	3.6	89.9	100.0				
Artrock5	refined (ESD[e])	3.1 (0.2)	5.4 (0.2)	0.7 (0.1)	5 (0.5)	85.7 (1.6)	100.0	10.4	2.6	0.3	
	difference	+1.8	+0.4	+0.5	+1.4	-4.2					8.3
	weighed (%)	5.4	5.0	1.1	5.0	83.5	100.0				
Artrock6	refined (ESD[e])	3.9 (0.2)	6.6 (0.2)	0.3 (0.1)	4.8 (0.5)	84.5 (1.9)	100.0	11.2	2.7	0.3	
	difference	+1.5	+1.6	-0.8	-0.2	+1.0					5.1
	weighed (%)	7.6	5.1	1.5	5.0	80.8	100.0				
Artrock7	refined (ESD[e])	3.7 (0.2)	6.1 (0.2)	0.3 (0.1)	5.5 (0.4)	84.5 (1.9)	100.0	11.6	2.8	0.3	
	difference	-3.9	+1.0	-1.2	+0.5	+3.7					10.3
	weighed (%)	10.9	3.0	2.2	5.0	78.9	100.0				
Artrock8	refined (ESD[e])	4.3 (0.2)	2.5 (0.1)	0.2 (0.1)	2.5 (0.3)	90.5 (3.0)	100.0	11.4	3.0	0.3	
	difference	-6.3	-0.5	-2.0	-2.5	+11.6					23.2

[a] Weighted pattern residual, a function of the least-squares residual (%).
[b] Reduced chi-squared statistic for the least-squares fit.
[c] Weighted Durbin-Watson statistic.
[d] Total bias (Δ) = $\sum$abs($W_{i,\,actual} - W_{i,\,reported}$), W_i is the weight% of the i^{th} mineral. (Omotoso et al., 2006).
[e] Estimated Standard Deviation, calculated using the Topaz V.5 "do_errors" macro.

This is a preprint, the final version is subject to change, of the American Mineralogist (MSA)
Cite as Authors (Year) Title. American Mineralogist, in press.
DOI: https://doi.org/10.2138/am-2018-6515

Table 4. Refinement results for Pawley/internal standard method

Sample	Abundance	Pyro-aurite	Magn-etite	Brucite	Hydrom-agnesite	Fluorite	Serpentine	Total	R_{wp}[a]	χ^2[b]	d[c]	Total bias[d]
	weighed (%)	1.7	6.4	1.0	0.9	10.0	80.0	100.0				
Artrock1	refined (ESD[e])	3.7 (0.2)	5.1 (0.2)	1.1 (0.1)	1.8 (0.6)	10.0 (0.0)	78.3 (0.6)	100.0	13.9	3.9	0.1	
	difference	+2.0	-1.3	+0.1	+0.9	+0.0	+1.7					6.6
	weighed (%)	2.9	4.5	1.6	4.5	10.0	76.5	100.0				
Artrock2	refined (ESD[e])	4.3 (0.2)	3.6 (0.2)	1.4 (0.1)	4.1 (0.6)	10.0 (0.0)	76.5 (0.7)	100.0	14.7	4.3	0.1	
	difference	+1.4	-0.9	-0.2	-0.4	+0.0	+0.0					3.3
	weighed (%)	2.9	4.5	1.6	9.0	10.0	72.0	100.0				
Artrock3	refined (ESD[e])	3.8 (0.1)	4.1 (0.1)	1.4 (0.1)	7.6 (0.4)	10.0 (0.0)	73.2 (0.5)	100.0	13.1	3.5	0.2	
	difference	+0.9	-0.4	-0.2	-1.4	+0.0	+1.2					4.6
	weighed (%)	3.0	4.5	1.6	13.5	10.0	67.4	100.0				
Artrock4	refined (ESD[e])	4.2 (0.2)	3.8 (0.2)	1.3 (0.2)	14.0 (0.8)	10.0 (0.0)	66.7 (0.9)	100.0	15.5	3.1	0.3	
	difference	+1.2	-0.7	-0.3	+0.5	+0.0	-0.7					3.9
	weighed (%)	1.2	4.5	0.2	3.2	10	80.9	100.0				
Artrock5	refined (ESD[e])	2.5 (0.3)	5.1 (0.2)	0.8 (0.3)	4.9 (1.0)	10.0 (0.0)	76.6 (1.1)	100.0	17.1	3.9	0.1	
	difference	+1.3	+0.6	+0.6	+1.7	+0.0	-4.3					9.6
	weighed (%)	4.9	4.5	1.0	4.5	10	75.2	100.0				
Artrock6	refined (ESD[e])	2.7 (0.2)	4.3 (0.2)	1.0 (0.2)	4.6 (0.6)	10.0 (0.0)	77.4 (0.7)	100.0	15.1	6.2	0.2	
	difference	-2.2	-0.2	+0.0	+0.1	+0.0	+2.2					5.3
	weighed (%)	6.8	4.6	1.4	4.5	10.0	72.7	100.0				
Artrock7	refined (ESD[e])	3.5 (0.2)	4.6 (0.2)	1.1 (0.2)	4.3 (0.5)	10.0 (0.0)	76.5 (0.6)	100.0	15.4	3.8	0.2	
	difference	-3.3	+0.0	-0.3	-0.2	+0.0	+3.8					8.6
	weighed (%)	9.8	2.7	2.0	4.5	10.0	71.0	100.0				
Artrock8	refined (ESD[e])	5.6 (0.2)	2.4 (0.2)	1.2 (0.3)	5.0 (0.6)	10.0 (0.0)	75.7 (0.8)	100.0	16.3	4.1	0.2	
	difference	-4.2	-0.3	-0.8	+0.5	+0.0	+4.7					11.9

[a] Weighted pattern residual, a function of the least-squares residual (%).
[b] Reduced chi-squared statistic for the least-squares fit.
[c] Weighted Durbin-Watson statistic.
[d] Total bias (Δ) = $\sum$abs($W_{i,\,actual} - W_{i,\,reported}$), W_i is the weight% of the i^{th} mineral. (Omotoso et al., 2006).
[e] Estimated Standard Deviation, calculated using the Topaz V.5 "do_errors" macro.

This is a preprint, the final version is subject to change, of the American Mineralogist (MSA)
Cite as Authors (Year) Title. American Mineralogist, in press.
DOI: https://doi.org/10.2138/am-2018-6515

Table 5. Refinement results for combined PONKCS-Pawley/internal standard method

Sample	Abundance	Pyro-aurite	Magne-tite	Brucite	Hydrom-agnesite	Fluorite	Serpentine	'Amorphous'	Total	R_{wp}[a]	χ^2[b]	d[c]	Total bias[d]
	weighed (%)	1.7	6.4	1.0	0.9	10.0	80.0		100.0				
Artrock1	refined (ESD[e])	2.8 (0.1)	3.5 (0.1)	0.8 (0.0)	0.8 (0.3)	10.0 (0.0)	88 (2.0)	-5.9 (1.8)	100.0	10.5	2.9	0.3	
	difference	+1.1	-2.9	-0.2	-0.1	+0.0	+8.0						12.3
	weighed (%)	2.9	4.5	1.6	4.5	10.0	76.5		100.0				
Artrock2	refined (ESD[e])	3.3 (0.1)	2.7 (0.1)	0.9 (0.1)	3.0 (0.3)	10.0 (0.0)	76.3 (1.9)	3.8 (1.9)	100.0	10.6	3.1	0.3	
	difference	+0.4	-1.8	-0.7	-1.5	+0.0	-0.2						4.6
	weighed (%)	2.9	4.5	1.6	9.0	10.0	72.0		100.0				
Artrock3	refined (ESD[e])	3.3 (0.1)	2.7 (0.1)	1 (0.1)	6.6 (0.4)	10.0 (0.0)	73.3 (1.6)	3.2 (1.6)	100.0	11.2	3	0.3	
	difference	+0.4	-1.8	-0.6	-2.4	+0.0	+1.3						6.5
	weighed (%)	3	4.5	1.6	13.5	10.0	67.4		100.0				
Artrock4	refined (ESD[e])	3.5 (0.2)	2.8 (0.1)	0.9 (0.1)	10.3 (0.5)	10.0 (0.0)	71.1 (1.7)	1.4 (1.7)	100.0	11.5	2.3	0.4	
	difference	+0.5	-1.7	-0.7	-3.2	+0.0	-3.7						9.8
	weighed (%)	1.2	4.5	0.2	3.2	10.0	80.9		100.0				
Artrock5	refined (ESD[e])	2.4 (0.3)	4.9 (0.2)	0.2 (0.1)	3.4 (0.4)	10.0 (0.0)	65.3 (2.0)	14.0 (1.7)	100.0	11	2.5	0.3	
	difference	+1.2	+0.4	+0.0	+0.2	+0.0	-15.6						17.4
	weighed (%)	4.9	4.5	1.0	4.5	10.0	75.2		100.0				
Artrock6	refined (ESD[e])	2.9 (0.2)	5.2 (0.2)	0.1 (0.1)	3.6 (0.3)	10.0 (0.0)	62.8 (1.7)	15.5 (1.4)	100.0	10.6	2.5	0.3	
	difference	-2.0	+0.7	-0.9	-0.9	+0.0	-12.4						16.9
	weighed (%)	6.8	4.6	1.4	4.5	10.0	72.7		100.0				
Artrock7	refined (ESD[e])	3.3 (0.2)	5.6 (0.2)	0.2 (0.1)	3.2 (0.4)	10.0 (0.0)	59.7 (2.1)	18.0 (1.7)	100.0	10.9	2.7	0.3	
	difference	-3.5	+1.0	-1.2	-1.3	+0.0	-13.0						20
	weighed (%)	9.8	2.7	2.0	4.5	10.0	71.0		100.0				
Artrock8	refined (ESD[e])	4.4 (0.2)	1.8 (0.1)	(0.1)	2.7 (0.3)	10.0 (0.0)	65.6 (1.9)	15.2 (1.7)	100.0	12.63	3.2	0.3	
	difference	-5.4	-0.9	-1.8	-1.8	+0.0	-5.4						15.3

[a] Weighted pattern residual, a function of the least-squares residual (%).
[b] Reduced chi-squared statistic for the least-squares fit.
[c] Weighted Durbin-Watson statistic.
[d] Total bias (Δ) = $\sum$abs($W_{i,\,actual} - W_{i,\,reported}$), W_i is the weight% of the i^{th} mineral. (Omotoso et al., 2006).
[e] Estimated Standard Deviation, calculated using the Topaz V.5 "do_errors" macro.

This is a preprint, the final version is subject to change, of the American Mineralogist (MSA)
Cite as Authors (Year) Title. American Mineralogist, in press.
DOI: https://doi.org/10.2138/am-2018-6515

Table 6. Estimated carbon sequestration plus carbonation potential (from brucite only) of artificial tailings

Sample	Method	Carbon sequestration potential (g CO_2)[a]				
		Hydrom-agnesite	Pyro-aurite	Brucite (Hydro)	Brucite (Pyro)	Total
Artrock1	Weighed	0.4	0.1	0.4	0.1	1.0
	PONKCS	0.4	0.2	1.0	0.2	1.7
	Pawley	0.7	0.2	0.4	0.1	1.4
	PONKCS-Pawley	0.3	0.2	0.3	0.1	0.8
Artrock2	Weighed	1.9	0.2	0.7	0.1	2.9
	PONKCS	1.7	0.3	0.4	0.1	2.5
	Pawley	1.5	0.3	0.5	0.1	2.4
	PONKCS-Pawley	1.1	0.2	0.4	0.1	1.8
Artrock3	Weighed	3.8	0.2	0.7	0.1	4.8
	PONKCS	3.0	0.3	0.5	0.1	3.9
	Pawley	2.8	0.2	0.5	0.1	3.7
	PONKCS-Pawley	2.5	0.2	0.4	0.1	3.1
Artrock4	Weighed	5.6	0.2	0.7	0.1	6.7
	PONKCS	4.3	0.3	0.5	0.1	5.1
	Pawley	5.3	0.3	0.5	0.1	6.1
	PONKCS-Pawley	3.9	0.2	0.3	0.1	4.5
Artrock5	Weighed	1.4	0.1	0.1	0.0	1.5
	PONKCS	1.9	0.2	0.3	0.0	2.4
	Pawley	1.9	0.2	0.3	0.1	2.4
	PONKCS-Pawley	1.3	0.2	0.1	0.0	1.5
Artrock6	Weighed	1.9	0.4	0.4	0.1	2.7
	PONKCS	1.8	0.3	0.1	0.0	2.2
	Pawley	1.7	0.2	0.4	0.1	2.4
	PONKCS-Pawley	1.3	0.2	0.0	0.0	1.6
Artrock7	Weighed	1.9	0.5	0.6	0.1	3.1
	PONKCS	2.1	0.2	0.1	0.0	2.4
	Pawley	1.6	0.2	0.4	0.1	2.3
	PONKCS-Pawley	1.2	0.2	0.1	0.0	1.5
Artrock8	Weighed	1.9	0.7	0.8	0.1	3.6
	PONKCS	1.0	0.3	0.1	0.0	1.3
	Pawley	1.9	0.4	0.5	0.1	2.8
	PONKCS-Pawley	1.0	0.3	0.1	0.0	1.4

[a] Total mass of each sample was 100 g.

This is a preprint, the final version is subject to change, of the American Mineralogist (MSA)
Cite as Authors (Year) Title. American Mineralogist, in press.
DOI: https://doi.org/10.2138/am-2018-6515

Figures

Figure 1

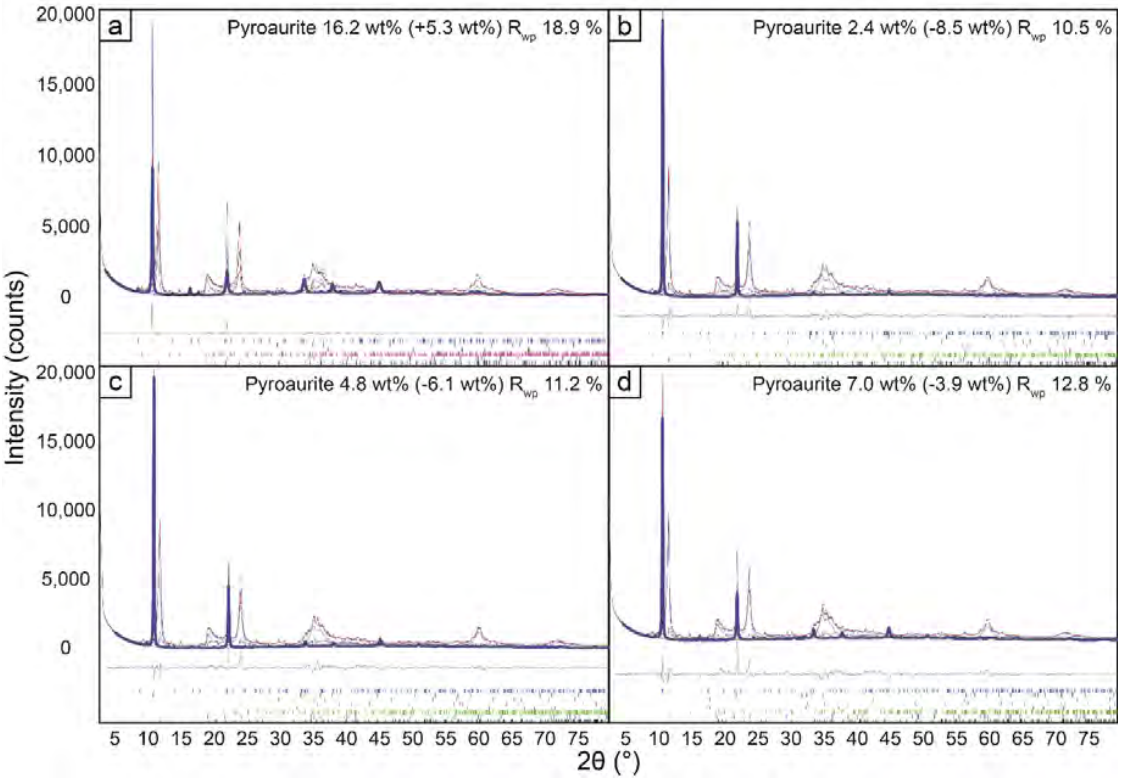

Figure 1. Modelling pyroaurite using with the PONKCS method and a) no March-Dollase preferred orientation, and a March-Dollase correction with b) no minimum value c) a minimum of 0.6 and d) a minimum of 0.75. Refined pyroaurite abundance (absolute error) and R_{wp} is reported for each of the conditions.

This is a preprint, the final version is subject to change, of the American Mineralogist (MSA)
Cite as Authors (Year) Title. American Mineralogist, in press.
DOI: https://doi.org/10.2138/am-2018-6515

Figure 2

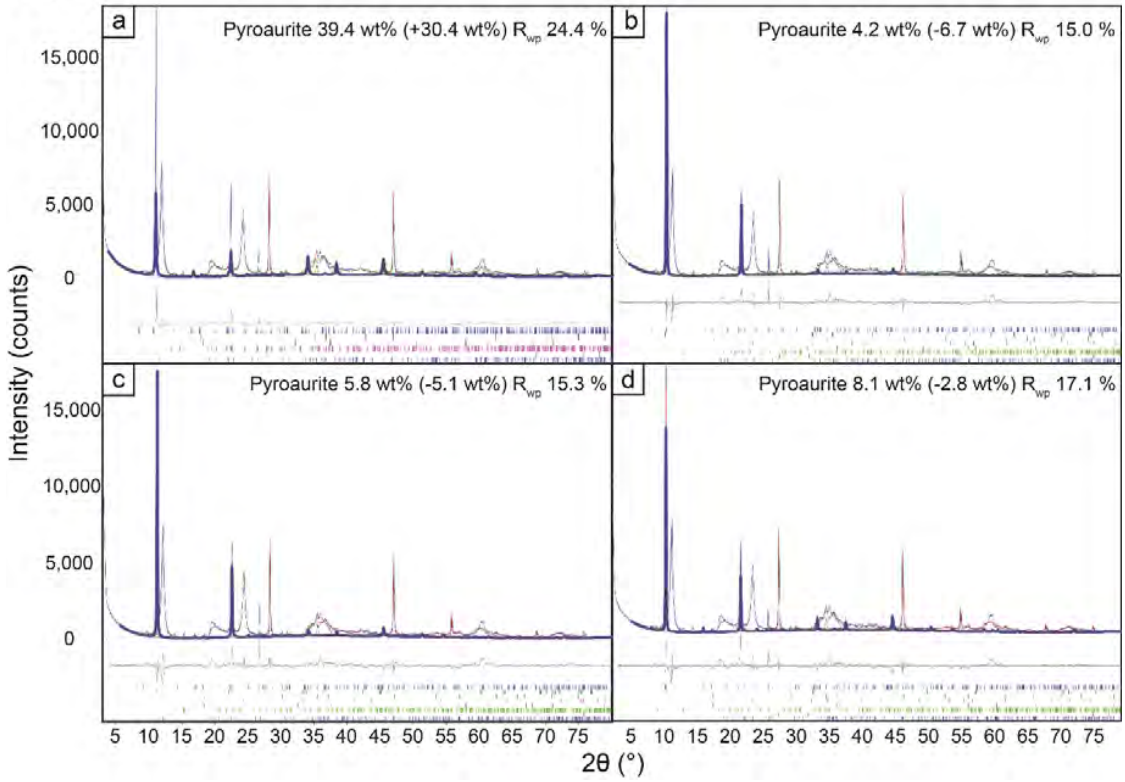

Figure 2. Modelling pyroaurite using with the Pawley/internal standard method and a) no March-Dollase preferred orientation, and a March-Dollase correction with b) no minimum value c) a minimum of 0.6 and d) a minimum of 0.75. Refined pyroaurite abundance (absolute error) and R_{wp} is reported for each of the conditions.

This is a preprint, the final version is subject to change, of the American Mineralogist (MSA)
Cite as Authors (Year) Title. American Mineralogist, in press.
DOI: https://doi.org/10.2138/am-2018-6515

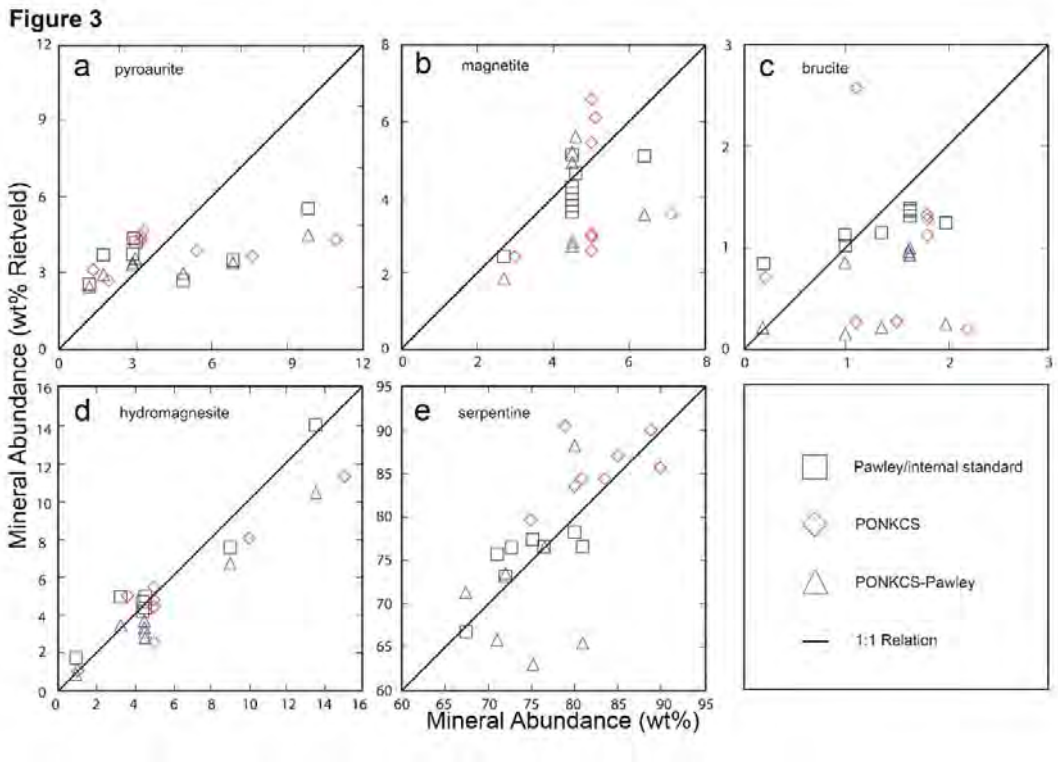

Figure 3. Results of Rietveld refinements for each mineral phase in the synthetic tailings using both the PONKCS and Rietveld spike method.

This is a preprint, the final version is subject to change, of the American Mineralogist (MSA)
Cite as Authors (Year) Title. American Mineralogist, in press.
DOI: https://doi.org/10.2138/am-2018-6515

Figure 4

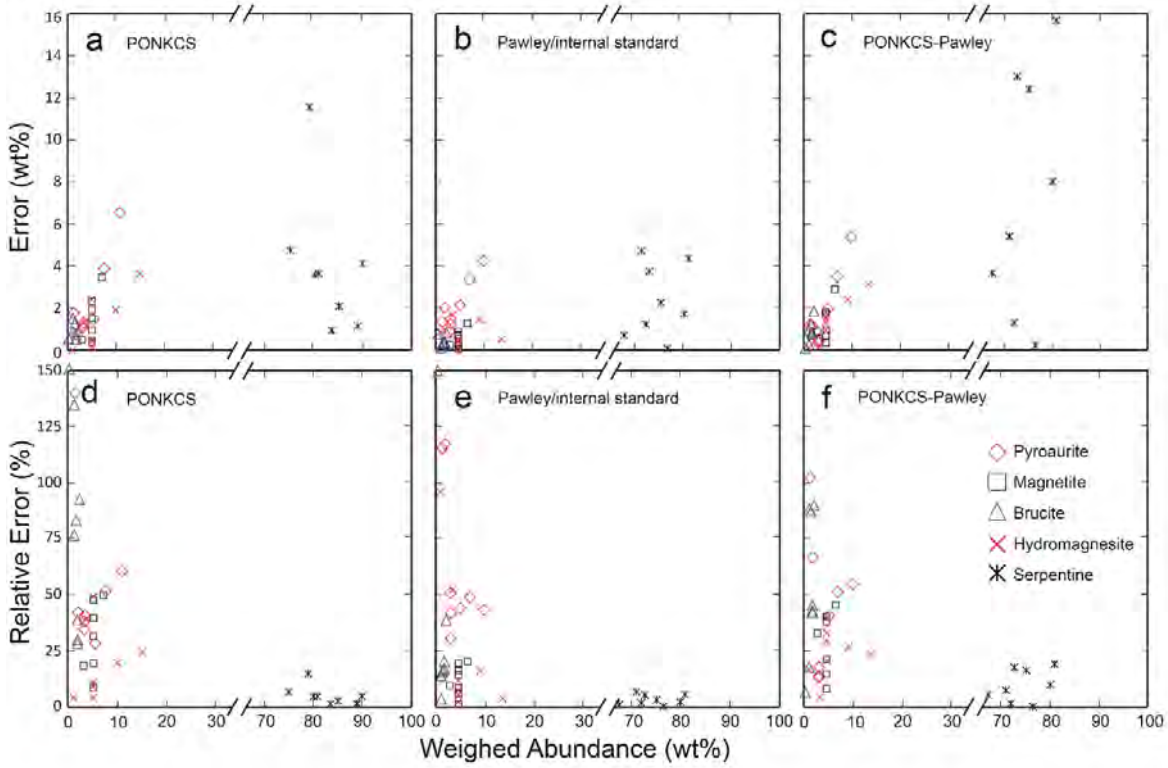

Figure 4. Relative and absolute error values between the weighed compositions of the artificial tailings samples and the compositions calculated via Rietveld refinement for a) absolute error values for PONKCS method b) relative error values for PONKCS method c) absolute error values for Rietveld spike method d) relative error values for Rietveld spike method.

This is a preprint, the final version is subject to change, of the American Mineralogist (MSA)
Cite as Authors (Year) Title. American Mineralogist, in press.
DOI: https://doi.org/10.2138/am-2018-6515

Figure 5

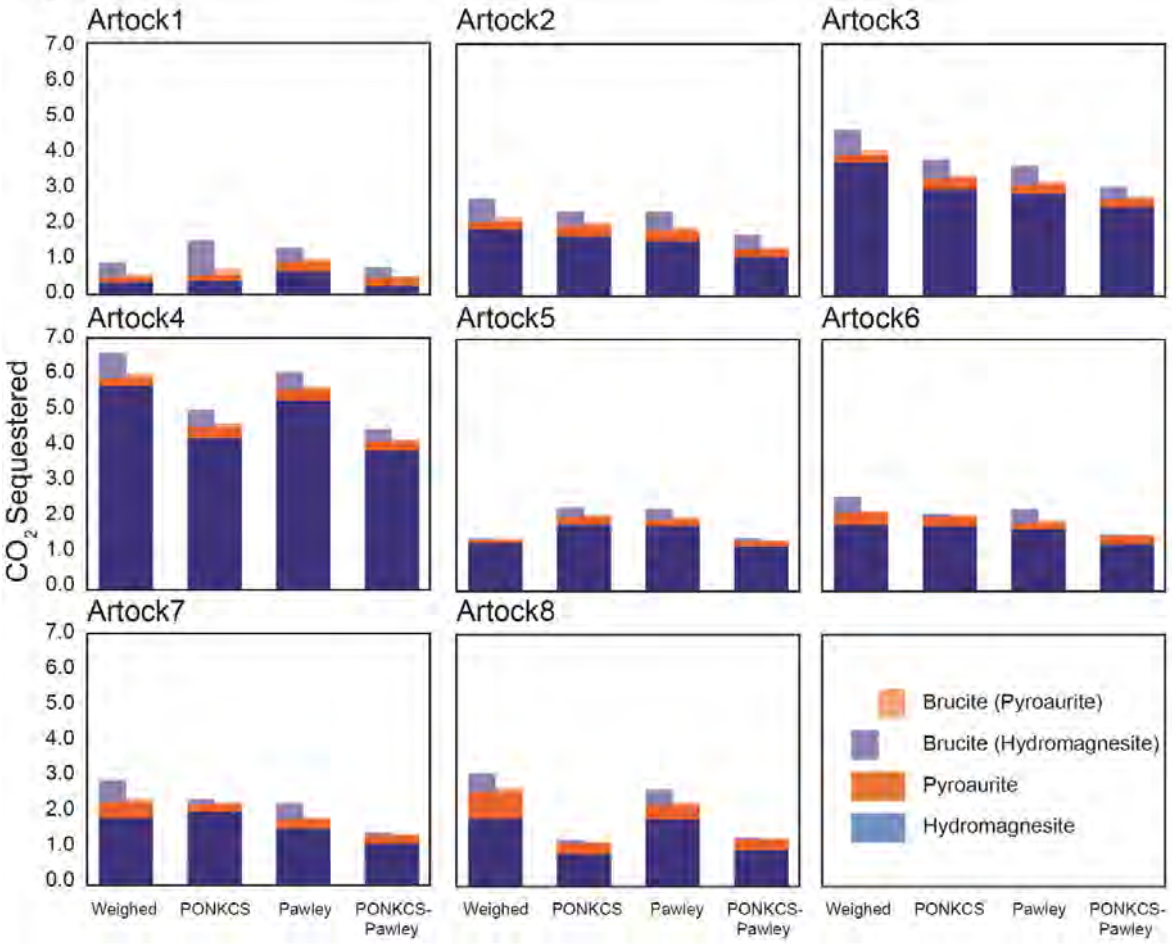

Figure 5. Estimates for carbon sequestration and remaining carbonation potential of the artificial tailings based on the abundance of (1) hydromagnesite and pyroaurite and (2) brucite, respectively according to their weighed and refined abundances. Two values are included for brucite to represent the potential for it to form hydromagnesite (high C) or pyroaurite (low C).